Painter, Stuart C.; Patey, Matthew D.; Forryan, Alexander; Torres-Valdes, Sinhue. 2013 Evaluating the balance between vertical diffusive nitrate supply and nitrogen fixation with reference to nitrate uptake in the eastern subtropical North Atlantic Ocean. *Journal of Geophysical Research: Oceans*, 118 (10). 5732-5749. 10.1002/jgrc.20416

Painter, Stuart C.; Patey, Matthew D.; Forryan, Alexander; Torres-Valdes, Sinhue. 2013 Evaluating the balance between vertical diffusive nitrate supply and nitrogen fixation with reference to nitrate uptake in the eastern subtropical North Atlantic Ocean. *Journal of Geophysical Research: Oceans*, 118 (10). 5732-5749. 10.1002/jgrc.20416

JOURNAL OF GEOPHYSICAL RESEARCH: OCEANS, VOL. 118, 5732–5749, doi:10.1002/jgrc.20416, 2013

Evaluating the balance between vertical diffusive nitrate supply and nitrogen fixation with reference to nitrate uptake in the eastern subtropical North Atlantic Ocean

Stuart C. Painter,[1] Matthew D. Patey,[2] Alexander Forryan,[3] and Sinhue Torres-Valdes[1]

Received 17 June 2013; revised 16 August 2013; accepted 25 September 2013; published 22 October 2013.

[1] The balance between N_2 fixation and diffusive NO_3^- supply is a key determinant for assessing the importance of both processes for new production in subtropical waters. Here we report observations of integrated N_2 fixation rates from the eastern subtropical North Atlantic Ocean with coincident estimates of diffusive NO_3^- supply. We find the average rate of N_2 fixation is equivalent to 62% of the diffusive NO_3^- supply, though N_2 fixation could exceed the diffusive flux at individual stations. Turbulent diffusivity measurements across the nitracline indicate a mean diffusivity of 0.077 $cm^2\ s^{-1}$. If approximations for methodological underestimates in the dominant N_2 fixation technique are considered, the magnitude of N_2 fixation is shown to represent 100% of the NO_3^- flux on average, and can be almost threefold higher at individual stations. As the study site is characterized by low rates of N_2 fixation compared to other sectors of the North Atlantic this confirms N_2 fixation as a major source term across the subtropical North Atlantic. The seasonal context of our observations suggests environmental factors underlie the in situ variability in observed N_2 fixation rates, and may well explain lower previous assessments of the importance of N_2 fixation relative to diffusive NO_3^- supply in this region. The diffusive NO_3^- supply provides $<20\%$ of measurable NO_3^- uptake with the remainder supplied via other mechanisms, most notably nitrification. The mean integrated rate of N_2 fixation equates to just 8% of the NO_3^- consumed on a daily basis by the phytoplankton community.

Citation: Painter, S. C., M. D. Patey, A. Forryan, and S. Torres-Valdes (2013), Evaluating the balance between vertical diffusive nitrate supply and nitrogen fixation with reference to nitrate uptake in the eastern subtropical North Atlantic Ocean, *J. Geophys. Res. Oceans*, *118*, 5732–5749, doi:10.1002/jgrc.20416.

1. Introduction

[2] The supply of externally sourced nutrients to the surface waters of subtropical oligotrophic gyres is a key control on overall levels of new production within such ecosystems. Historically, the presence of persistent water column stratification and the absence of strong convective mixing focused attention upon the vertical diffusive flux of NO_3^- as the primary pathway by which NO_3^- (and hence new nutrients) reached the surface ocean. The validity of this statement appeared confirmed when *Lewis et al*. [1986] found a general agreement (to within an order of magnitude) between rates of integrated NO_3^- uptake and of diffusive NO_3^- supply across the nitracline. In the period since this important study was published it has been recognized that the diffusive flux of nutrients is augmented by other sporadic inputs such as those provided by mesoscale eddies, internal waves, and atmospheric deposition (reviewed by *Lipschultz et al*. [2002]). The identification and quantification of these multiple nutrient supply pathways remains a major research objective, particularly given existing imbalances between rates of production that can be supported by directly measured nutrient supply terms and the higher rate of production indirectly inferred by geochemical methods [*Jenkins*, 1982].

[3] Alongside developments in our understanding and quantification of the physical mechanisms that supply nutrients to the surface ocean has been improved recognition of the role of diazotrophy in injecting new nitrogen into the surface ocean. N_2 fixation has now moved from being viewed as a relatively unimportant process [*Dugdale and Goering*, 1967] to one that occupies a central role in our conceptual view of nutrient cycling within the ocean [*Gruber*, 2008]. In particular, the importance of diazotrophic organisms for new and export production is increasingly recognized [*Karl et al*., 1997, 2002, 2012; *Capone et al*., 2005;

[1]National Oceanography Centre, European Way, Southampton, Hampshire, UK.
[2]Chemistry Department, Universidad de Las Palmas de Gran Canaria, Las Palmas de Gran Canaria, Spain.
[3]National Oceanography Centre, School of Ocean and Earth Science, University of Southampton, Waterfront Campus, European Way, Southampton, Hampshire, UK.

Corresponding author: S. C. Painter, National Oceanography Centre, European Way, Southampton, Hampshire SO14 3ZH, UK. (stuart.painter@noc.ac.uk)

2169-9275/13/10.1002/jgrc.20416

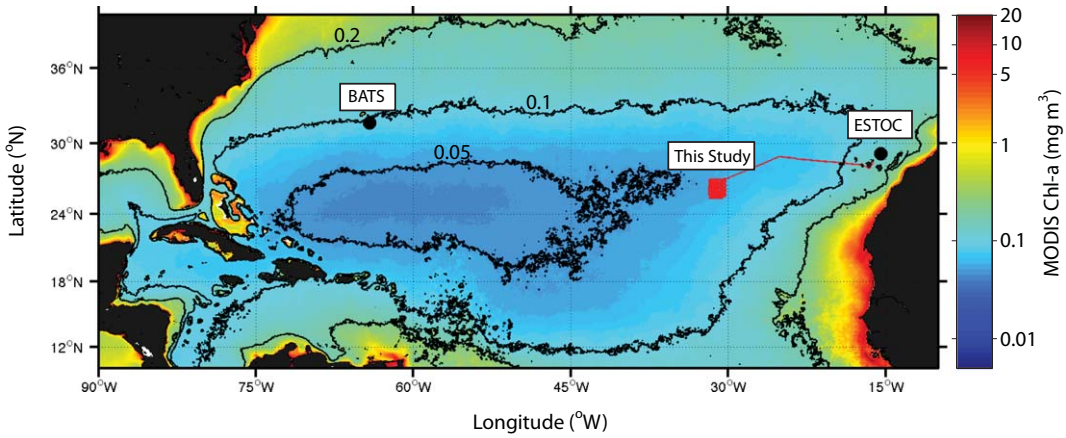

Figure 1. Cruise transect and survey region (red square) shown in relation to the wider subtropical North Atlantic and established time-series study sites including Bermuda Atlantic Time Series (BATS) and the European Station for Time Series in the Ocean (ESTOC). The underlying surface chlorophyll image is the MODIS Aqua mission average for the period 2002–2011. Selected contours (as labeled) are presented to show the long-term mean position of the North Atlantic subtropical gyre.

Carpenter and Capone, 2008; *Karl and Letelier*, 2008]. At the global scale active debate over the balance between N_2 fixation and denitrification, the major oceanic loss term for fixed N, suggests that the marine N cycle is largely balanced [*Gruber and Sarmiento*, 1997; *Capone et al*., 2005; *Deutsch et al*., 2007; *Gruber*, 2008; *DeVries et al*., 2012]. However, the relevance of regional variability in N_2 fixation rates is still not properly understood.

[4] Areal estimates of N_2 fixation rates have been shown to rival or exceed in magnitude the diffusive flux of NO_3^- [*Capone et al*., 2005; *Mahaffey et al*., 2005]. The balance between these two supply processes, however, is spatially and temporally variable. Consequently, direct measurement of both processes is required to validate such conclusions and to identify regions of the ocean where N_2 fixation may be quantitatively more important. Surprisingly, it appears that only recently have the rates of diffusive NO_3^- supply and of N_2 fixation been compared simultaneously [*Mourino-Carballido et al*., 2011]. Previous comparisons, particularly for basin scale syntheses, have often been made on the basis of an assumed turbulent diffusivity (Kz), such as that obtained by *Ledwell et al*. [1993] (i.e., Kz = 0.11 cm^2 s^{-1}), which is assumed to be broadly constant in space and time. Nevertheless, even with this assumption in place areal rates of N_2 fixation have been shown to represent significant inputs of new nitrogen, which suggests that unless diffusivities are considerably more heterogeneous than currently thought the general conclusion that N_2 fixation can exceed diffusive NO_3^- supply is indeed valid in certain cases. However, limited understanding of the spatiotemporal variability in N_2 fixation rates away from the tropical belt of maximum N_2 fixation means that it is unclear if the dominance of N_2 fixation over the diffusive NO_3^- supply can be considered typical.

[5] Despite general conclusions regarding the importance of N_2 fixation, *Mourino-Carballido et al*. [2011] found that N_2 fixation represented between 2% and 44% of the diffusive NO_3^- flux in the subtropical North and South Atlantic, respectively. The low contribution for the North Atlantic seems to be at odds with the broader distribution and importance of diazotrophy across the North Atlantic [*Capone et al*., 2005; *Carpenter and Capone*, 2008] and its implied impact upon the distribution of N* [*Gruber and Sarmiento*, 1997; but see also *Singh et al*., 2013]. This may indicate an important spatial decoupling between the two supply processes, indicate some facet of regional or seasonal variability that we poorly understand or possibly indicate that the true significance of N_2 fixation for new production is equally poorly understood [*Singh et al*., 2013].

[6] The eastern subtropical North Atlantic is characterized by relatively low rates of N_2 fixation compared to the western North Atlantic and equatorial regions [*Capone et al*., 2005; *Carpenter and Capone*, 2008; *Subramaniam et al*., 2013] and detailed assessments of the importance of N_2 fixation versus diffusive NO_3^- supply for overall productivity levels are lacking. Here we address these omissions and present measurements of primary production, NO_3^- uptake, and N_2 fixation from the eastern subtropical North Atlantic along with simultaneous estimates of the vertical diffusive NO_3^- supply to critically evaluate the importance of N_2 fixation relative to the NO_3^- supply.

2. Methods

2.1. Cruise Overview and Environmental Characterization

[7] All data were collected between 11 August and 12 September 2011 at a nominal location of 26.5°N, 29.5°W (Figure 1). All CTD casts were located within a 160 km radius around this position and conducted during repeated mesoscale surveys of the area. Water sample collection and environmental characterization were performed using a Seabird 9/11+ CTD-Niskin rosette package. Mixed layer depths were estimated using a density threshold criterion of 0.03 kg m^{-3} relative to the density at 10 m [*de Boyer Montegut et al*., 2004]. Mixed layer depths were generally deeper (20–60 m) between 11 August and 25 August than they were subsequently (<30 m), and the cruise mean mixed layer depth was 28 ± 15 m.

[8] The depth of the euphotic zone (0.1% surface irradiance) was derived from knowledge of the water column attenuation coefficient (K_d), which was estimated from a regression of log normalized irradiance intensity (PAR; photosynthetically active radiation) against depth. PAR data were collected from a CTG 2π PAR sensor fitted to the CTD frame and only casts conducted around local noon (± 3 h) were used in this assessment, which resulted in an average K_d for the cruise of 0.044 ± 0.002 (range 0.041–0.048) and produced a cruise average euphotic zone depth of 158 ± 7 m; comparable to the deepest chlorophyll maximum (DCM) we observed.

2.2. Biological and Chemical Variables

[9] Discrete chlorophyll concentrations were estimated fluorometrically from 250 ml or 500 ml seawater samples filtered onto 25 mm Whatman GF/F (0.7 μm pore size) glass fiber filters and extracted in 90% acetone at 4°C overnight (16–20 h). Chlorophyll extracts were measured following the method of *Welschmeyer* [1994] using a Turner Trilogy fluorometer calibrated against a pure chlorophyll-*a* standard (spinach extract—Sigma Aldrich). CTD fluorescence profiles were calibrated against the discrete chlorophyll samples using linear regression analysis. The calibration equation $y = 2.5766x - 0.0124$ ($R^2 = 0.93$, $n = 196$), where y is the calibrated fluorescence profile (mg m^{-3}) and x is the measured chlorophyll concentration (mg m^{-3}), was applied to all fluorescence profiles.

[10] Water samples for the determination of total nitrate ($NO_3^- + NO_2^-$, hereafter NO_3^-), phosphate (PO_4^{3-}) and orthosilicic acid ($Si(OH)_4$) concentration were drawn directly from CTD Niskin bottles into clear polystyrene vials and analyzed immediately or stored in the dark at 4°C whilst awaiting analysis. All concentrations were determined colorimetrically using a 3 channel Skalar Sanplus autoanalyser following the methods described by *Kirkwood* [1996]. Detection limits of better than 0.1 μmol L^{-1} for NO_3^- and $Si(OH)_4$ and 0.01 μmol L^{-1} for PO_4^{3-} were achieved throughout. As these detection limits were insufficient for the oligotrophic waters of the study site, we also measured NO_3^- and PO_4^{3-} concentrations at nanomolar levels using the liquid capilliary waveguide methodology described by *Patey et al*. [2008, 2010]. This provided a limit of detection of around 0.5 nmol L^{-1} for both NO_3^- and PO_4^{3-}.

2.3. ^{13}C, $^{15}NO_3^-$, and $^{15}N_2$ Fixation Rate Measurements

[11] Water samples were collected from five depths across the euphotic zone for the measurement of primary production, NO_3^- uptake, and N_2 fixation. Sampling depths were chosen based on irradiance levels and represented 97, 55, 33, and 14% of surface irradiance intensity with an additional sample from the depth of the DCM (<1% PAR). For the measurement of primary production and NO_3^- uptake, duplicate 2 L water samples from each depth were carefully measured into clean Nalgene polycarbonate bottles and dual labeled with $Na^{13}CO_3^-$ and $K^{15}NO_3^-$. The ^{13}C label (99% enriched, CIL Laboratories) was added at a fixed concentration of 105 μmol L^{-1}, equating to 5% of the available dissolved inorganic carbon (DIC) pool (~2100 μmol L^{-1}), whereas the $^{15}NO_3^-$ label (99.5% enriched) was added at a variable concentration of between 1 and 5 nmol L^{-1} to take into account both spatial and vertical changes in the ambient NO_3^- concentration. These additions represent on average $16 \pm 9\%$ of the ambient NO_3^- concentration but in individual bottles the tracer addition varied from <1 to 50% of the actual NO_3^- concentration; thus whilst our results broadly reflect natural conditions they are a combination of trace and saturated uptake rates.

[12] Samples from the 97–14% irradiance depths were incubated using on-deck incubators shielded to appropriate irradiance levels with optical filters (210 0.6 Neutral Density and 061 Mist Blue; Lee Filters) and flushed with running seawater collected from ~5 m depth (~24°C). Bottles from the deepest sampling depths were incubated using a FytoScope FS130 plant growth chamber (Photon Systems Instruments, www.psi.cz), which allowed precise temperature and irradiance control (cool white LEDs). The temperature within the growth chamber was set to 17°C reflective of in situ temperatures, whilst the irradiance level was set to ~7 μmol photons m^{-2} s^{-1} which was previously determined to approximate peak daily irradiance intensities at the depth of the DCM. Confirmation of this approximation was gained from a retrospective analysis of ship measured total daily incident PAR, which ranged from 22.5 to 60 mols photons m^{-2} d^{-1} and averaged 50.6 ± 10.6 mols photons m^{-2} d^{-1} over the period of the cruise. The daily irradiance cycle at the DCM was estimated following *Kirk* [2010] using a transmission coefficient of 0.98 and the cruise average attenuation coefficient of 0.044 m^{-1}. Calculated in this way, the average daily maximum irradiance intensity at the DCM was 6.8 ± 1.2 (range 3.2–8) μmol photons m^{-2} s^{-1} (Figure 2), whereas the daily average PAR experienced by the DCM was 1.9 ± 0.4 μmol photons m^{-2} s^{-1} (Figure 2). The daily integrated PAR received by the DCM averaged 0.17 ± 0.04 (range 0.08–0.2) mols photons m^{-2} d^{-1}.

[13] All samples were incubated for 4–6 h before gentle filtration onto ashed (>6 h 450°C) 25 mm Whatman GF/F filters (0.7 μm pore size). Filters were stored frozen at −20°C onboard. Once back in the laboratory all filters were dried overnight at 40°C, pelleted into tin capsules using a laboratory press and analyzed by mass spectrometry for particulate and isotopic N and C content. Uptake rates (units nmol L^{-1} h^{-1}) were calculated using the equations of *Dugdale and Wilkerson* [1986]. ^{13}C uptake rates were calculated assuming an ambient DIC concentration of 2100 μmol C L^{-1} (=25.2 mg C L^{-1}) and using a ^{13}C natural abundance of 1.0790%, which was the mean value obtained from the isotopic analysis of independent samples collected for measurements of particulate organic carbon (POC)/particulate organic nitrogen (PON) concentration and T_0 initial isotopic conditions as part of the N_2 fixation experiments.

[14] N_2 fixation rates were measured using the method described by *Montoya et al*. [1996] for both total and <8 μm size fractions (samples were prefiltered). The <8 μm size fraction was included to provide an indication of diazotrophy by the unicellular component of the plankton community. At each sampled depth and for each size fraction, a 4.2 L polycarbonate bottle was filled to the brim and closed with a gas tight septum cap taking care to remove all air bubbles first. Once sealed, 4 ml of 99% $^{15}N_2$ gas were injected through the septum and the bottle

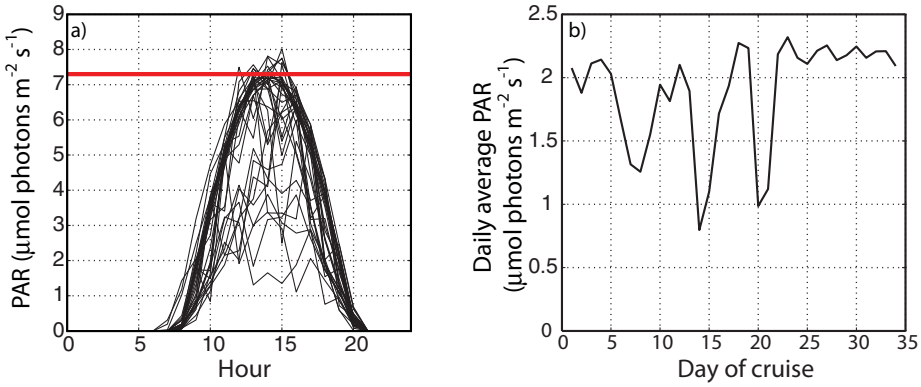

Figure 2. (a) Calculated daily irradiance cycles for the deep chlorophyll maximum where peak daily irradiance intensity averaged 6.8 ± 1.2 μmol photons m^{-2} s^{-1}. The red line indicates the irradiance intensity setting of the Fytoscope incubator (~7 μmol photons m^{-2} s^{-1}) used in this study for samples collected from the deep chlorophyll maximum. (b) Daily average irradiance at the deep chlorophyll maximum with a cruise average of 1.9 ± 0.4 μmol photons m^{-2} s^{1}.

rolled from side-to-side for several minutes to aid equilibration of the tracer with the dissolved N_2 gas content of the sample. All bottles were incubated for 24 h using the same incubators as described above, though incubators were covered/LED's turned off at night to protect samples from the ship's lights. All samples were filtered under gentle vacuum pressure onto ashed 25 mm Whatman GF/F filters, which were then stored frozen at −20°C for return to the laboratory where filters were dried and pelleted for analysis. N_2 fixation rates (nmol L^{-1} d^{-1}) were calculated using the mass balance equations detailed in *Montoya et al*. [1996].

[15] To provide daily integrals of carbon fixation and of NO_3- uptake from our subdaily incubations to compare to the daily rates of N_2 fixation, we have scaled the hourly carbon uptake rates by the standard solar day length (12 h) and hourly NO_3^- uptake rates by 18 h to account for dark NO_3^- uptake, which may be significant [*Mulholland and Lomas*, 2008]. In doing this, we have assumed that dark NO_3^- uptake occurs at a rate equivalent to 50% of that observed in the daylight [*Mulholland and Lomas*, 2008].

2.4. Turbulence Measurements and Diffusive Nitrate Fluxes

[16] Turbulent kinetic energy dissipation (ε) was measured at 13 stations during the cruise from microstructure velocity shear measurements collected using an MSS90L free-fall microstructure shear profiler produced by Sea and Sun Technology GmbH and ISW Wassermesstechnik using the methodology described by *Forryan et al*. [2012, 2013]. Briefly, turbulent diffusivity is related to the dissipation of turbulent kinetic energy [*Osborn*, 1980; *Moum et al*., 1995; *Rippeth et al*., 2003] and under conditions of isotropic turbulence [*Yamazaki and Osborn*, 1990] the rate of turbulent kinetic energy dissipation can be calculated from the variance of the measured vertical microstructure shear by integration of the vertical microstructure shear power spectrum [*Moum et al*., 1995; *Rippeth et al*., 2003; *Stips*, 2005]. The microstructure shear power spectrum was estimated using the modified periodogram method [*Welch*, 1967] from the vertical microstructure shear fluctuations. This power spectrum was then used to calculate the rate of turbulent diffusivity (*Kz*) as described by *Forryan et al*. [2012, 2013].

[17] Due to the limited number of stations at which turbulent diffusivity was measured (13) we have calculated the geometric mean diffusivity profile that we use to estimate diffusive NO_3^- fluxes. This was achieved by first log transforming the diffusivity data prior to averaging. We then subsequently averaged the diffusivity measurements between 90 and 160 m depth (i.e., across the nitracline) to obtain the diffusivity term *Kz*. Vertical diffusive NO_3^- fluxes were calculated at the top of the nitracline using a concentration of 100 nmol NO_3^- L^{-1} to signify this position and at the depth of the maximum nitracline gradient using a common methodology. In both cases, the local NO_3^- gradient $\left(\frac{\partial NO_3}{\partial z}\right)$ was obtained via linear interpolation, and combined with the mean diffusivity term (*Kz*) via the equation $\left(Kz\ \frac{\partial NO_3}{\partial z}\right)$ to produce diffusive flux estimates.

3. Results

3.1. Environmental Context

[18] We present in Figure 3 a time series of observations for the upper 200 m of the water column under the assumption that spatial differences due to the geographic positioning of individual CTD casts is less influential than the regional temporal trend. The hydrographic conditions characterized by the contour plots of temperature, salinity, and density reveal that near surface waters (<30 m) increased in temperature by ~2.5°C from ~23.1°C to >25.7°, surface salinity increased by 0.35 from 37.24 to 37.59 and there was a coincident decrease in surface density of 0.58 kg m^{-3} from 25.59 to 25.01 kg m^{-3} over the period of observation. Below 50 m depth there was less temporal variability but a number of shallower isotherms, isohalines and isopycnals progressively deepen suggesting that the changes we observe slowly spread throughout the euphotic zone. Seasonal heating may indeed play a role in some of these near surface changes (see section 3.5) but the magnitude of change is often far larger than would be expected by this process alone thus the most likely explanation must also involve a degree of spatial variability. Within the

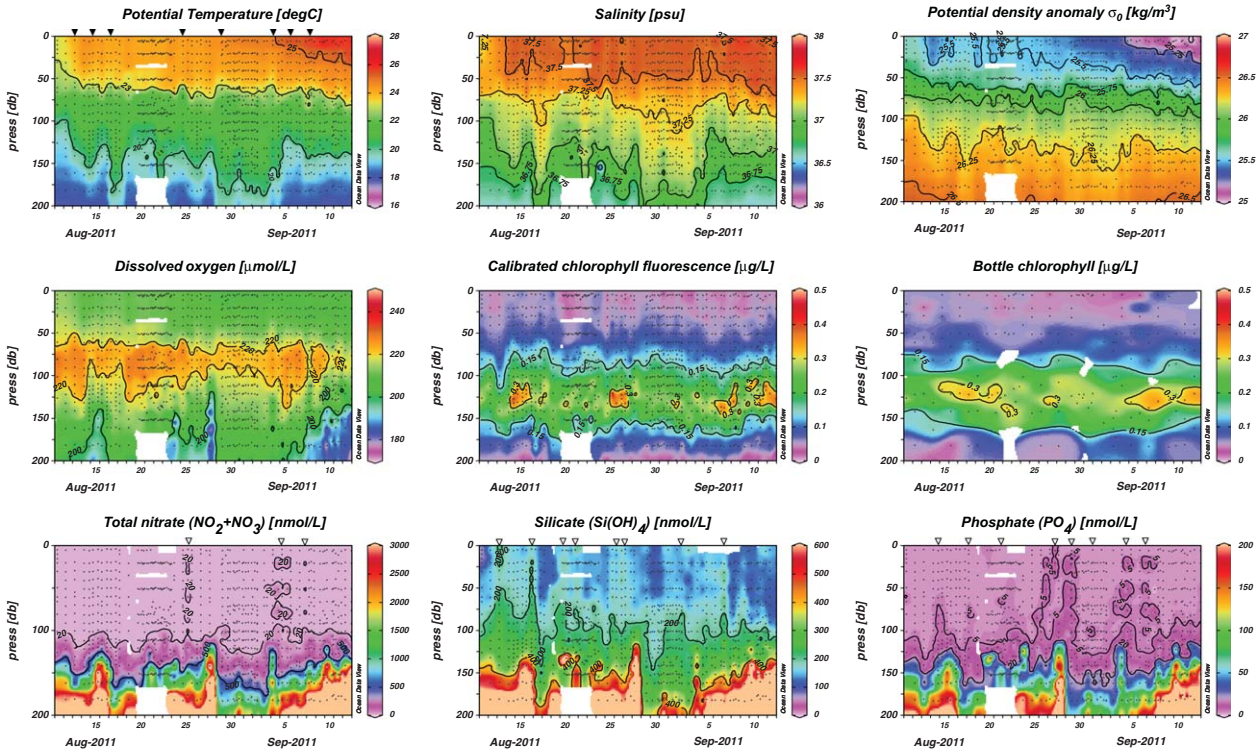

Figure 3. Time-series plots of environmental conditions during the cruise (a) potential temperature, (b) salinity, (c) density, (d) dissolved oxygen, (e) calibrated chlorophyll fluorescence, (f) bottle chlorophyll, (g) total nitrate, (h) orthosilicic acid ("silicate"), and (i) phosphate. Note that the hydrographic data are based upon a reduced data set of bottle stop observations so as to present a similar vertical resolution as the other parameters. The black triangles along the top of the potential temperature section indicate sampling periods for the rate measurements reported here. The white triangles along the top of the nutrient sections indicate nutrient injection events.

thermocline (~150 m) isotherms can be seen to oscillate vertically by up to 50 m, which is most likely due to undulations within the thermocline in response to physical forcing (instabilities, internal waves, etc).

[19] Dissolved oxygen profiles, which highlight an important region of primary production, show a persistent subsurface oxygen maximum located at a mean depth of 80 ± 8 m (range 53–99 m) (Figure 3). Maximum oxygen concentrations on individual profiles varied from 226 to 241 µmol L^{-1} (mean 233 ± 3 µmol L^{-1}) and whilst peak oxygen concentrations appear to decrease with time, the subsurface oxygen maximum remained clearly visible in all individual profiles.

[20] We also present in Figure 3 calibrated fluorescence and bottle chlorophyll data. The depth of the DCM was identified from calibrated chlorophyll fluorescence profiles and found to vary in depth from 105 to 159 m with a cruise average of 129 ± 11 m, some 50 m deeper than the mean depth of the oxygen maximum [as is typical for subtropical waters *Hayward*, 1991, 1994]. Maximum chlorophyll concentrations at the DCM were 0.3–0.4 µg L^{-1}, though there could be considerable variability in the maximum chlorophyll concentration observed between profiles indicating significant heterogeneity within the DCM. Chlorophyll concentrations >0.15 µg L^{-1} were observed between 75 and 175 m depth and elevated relative to surface concentrations (~0.05 µg L^{-1}), resulting in a rather broad feature but at its core the DCM was a rather more abrupt feature usually <10 m thick. Despite repeated sampling only a weak and insignificant correlation between the depth of the DCM and of the 1% irradiance depth was identified. This correlation was far weaker than is widely assumed and resulted from the DCM occupying a deeper position relative to the depth of the 1% isolume at most stations. Using the average attenuation coefficient for the cruise (0.044 m^{-1}), we calculate that the DCM was located at a mean irradiance intensity of 0.39% of surface irradiance and comparable to the 0.26% level identified by *Venrick et al*. [1973] in the North Pacific.

[21] Nutrient concentrations are also shown in Figure 3. NO_3^- concentrations were consistently at nanomolar levels (<10 nmol L^{-1}) throughout the upper 100 m of the water column (mean concentration 7.1 ± 1.8 nmol L^{-1}) and increased below 100 m depth signifying the position of the nitracline. The nitracline, defined here by a concentration of 100 nmol L^{-1}, was located at a mean depth of 129 ± 13 m but found to vary from 95 to 160 m on individual profiles. Silicate concentrations were typically <200 nmol L^{-1} in the upper 100 m of the water column (mean 164 ± 87 nmol L^{-1}), but Si concentrations proved to be rather variable resulting in a patchy distribution and regions with Si concentrations <100 nmol L^{-1} could be discerned. The patchy nature of surface silicate concentrations is reflected in the position of deeper isopleths, which are shoaler when

Table 1. Summary of Station Positions, Integration Depths, and Integrated (Trapezoidal Method) State Variables and Biological Uptake Rates

Station	Date	Latitude (N)	Longitude (W)	Integration Depth (m)	Integrated chl-*a* (mg m^{-2})	Integrated NO_3^- (mmol NO_3^- m^{-2})	Integrated Production (mmol C m^{-2} d^{-1})	Integrated ρNO_3^- (mmol N m^{-2} d^{-1})	Total Integrated N_2 Fixation (μmol N m^{-2} d^{-1})	<8 μm Integrated N_2 Fixation (μmol N m^{-2} d^{-1})
1	13/08/11	27.0022	30.2984	121	9.27	1.00	14.86	0.13	15.35	10.29
2	15/08/11	25.7964	31.1772	116	16.86	3.15	32.47	0.57	27.74	11.07
3	17/08/11	26.4469	31.0652	120	17.63	0.72	21.66	0.38	21.98	8.36
4	25/08/11	26.9946	30.3484	144	16.81	10.49	24.57	0.77	33.13	8.99
5	29/08/11	26.6028	31.3435	123	15.11	1.48	28.42	0.62	16.78	
6	04/09/11	26.0977	31.8269	111	13.07	1.26	19.36	0.40	95.62	
7	06/09/11	26.7296	30.9711	144	20.42	17.95	22.53	0.74	20.45	
8	08/09/11	25.3992	31.2602	130	20.18	5.57	26.95	1.18	63.30	

surface concentrations are higher and are deeper when they are lower, suggesting that this variability in surface Si concentrations is related to activity within the thermocline [*Bibby and Moore*, 2011]. Finally, PO_4^{3-} concentrations were typically <5 nmol L^{-1} in the upper 100 m (mean 3.2 ± 0.9 nmol L^{-1}) and a little higher than reported for the western subtropical North Atlantic (0.2–1 nmol L^{-1}) [*Wu et al*., 2000], but increased with depth. Concentrations >10 nmol L^{-1} were typically encountered below 120 m depth, but there is clearly some variability between stations including what may very well be a number of eutrophication events when pockets of water with $PO_4^{3-} > 5$ nmol L^{-1} were identified within the upper 100 m (Figure 3). We have used an arbitrary concentration of 100 nmol PO_4^{3-} L^{-1} to signify the position of the phosphocline, recognizing that this may overestimate the actual depth given the generally lower concentration of PO_4^{3-} relative to NO_3^-. In this way, we obtain a mean phosphocline depth of 177 ± 27 m, roughly 40 m deeper than the corresponding nitracline but supportive of the general observation of a vertical decoupling between the nitracline and phosphocline within the Atlantic Ocean [*Longhurst and Harrison*, 1989].

3.2. Rate Measurements

[22] Rates of carbon fixation varied from 0.6 to 29.3 nmol C L^{-1} h^{-1} (0.007–0.35 mmol C m^{-3} d^{-1}) with maximum rates located in surface waters (upper 30 m) and decreasing below this. Daily integrated production (Table 1) ranged from 14.9 to 32.5 mmol C m^{-2} d^{-1}, very similar to previous measurements of primary production rates in these waters [*Maranon et al*., 2000; *Poulton et al*., 2006; *Perez et al*., 2006].

[23] Rates of NO_3^- uptake (ρNO_3^-) varied from 0.03 to 1.17 nmol N L^{-1} h^{-1}. In general, ρNO_3^- rates remained relatively uniform or decreased with depth, which is consistent with both the NO_3^- impoverished nature of these waters and the reduction in irradiance intensity with depth. Given the sampling resolution, there is minimal evidence for any enhancement in ρNO_3^- at depth around the nitracline as reported previously [*Le Bouteiller*, 1986; *Eppley and Koeve*, 1990; *Harrison* 1990; *Painter et al*., 2007]. Daily-integrated ρNO_3^- rates ranged from 0.13 to 1.18 mmol N m^{-2} d^{-1} (Table 1) and were very comparable to previous observations from this region (see section 4).

[24] Rates of N_2 fixation were generally <0.5 nmol N L^{-1} d^{-1} throughout the water column with isolated enhancements of up to 2.8 nmol N L^{-1} d^{-1} at the shallowest sampled depths. N_2 fixation rates in the <8 μm fraction were noticeably lower peaking at just 0.24 nmol N L^{-1} d^{-1}, and unlike the vertical profiles for the total fraction, a small yet distinct peak in N_2 fixation by the <8 μm fraction was evident between 20 and 30 m. Daily-integrated N_2 fixation rates ranged from 15.4 to 95.62 μmol N m^{-2} d^{-1} for the full size fraction and from 8.36 to 11.07 μmol N m^{-2} d^{-1} for the <8 μm fraction (Table 1). The composition of the diazotrophic community, particularly in the <8 μm fraction, is unknown but a large and exceptional bloom of *Trichodesmium* was encountered during this cruise which was clearly visible from the ship and we consider the larger diazotroph fraction to have been *Trichodesmium* dominated.

Table 2. Comparison of Turbulent Diffusive NO_3^- Supply Calculated at the Top of the Nitracline (=100 nmol NO_3^- L^{-1}) and at the Depth of the Maximum Nitracline Gradient With Local Integrated NO_3^- Uptake

			Kz (cm^2 s^{-1}) = 0.077			
Station	NO_3^- Uptake (μmol N m^{-2} d^{-1})	Nitracline Gradient (μmol m^{-4})	NO_3^- Flux (μmol m^{-2} d^{-1})	Flux as % of Uptake	N_2 Fix as % of Flux	N_2 Fix as % of ρNO_3
Top of Nitracline						
1	134.3	18.76	12.48	9.3	123	11
2	574.0	12.64	8.41	1.5	330	5
3	383.3	5.48	3.65	1.0	602	6
4	773.3	16.95	11.28	1.5	294	4
5	618.1	11.12	7.40	1.2	227	3
6	399.6	44.50	29.61	7.4	323	24
7	735.5	26.01	17.30	2.4	118	3
8	1175.3	12.37	8.23	0.7	769	5
Mean ± standard deviation	599.2 ± 312.7	18.5 ± 12.1	12.3 ± 8.1	3.1 ± 3.3	348 ± 228	8 ± 7
Maximum Nitracline Gradient						
1	134.3	129.42	86.10	64.1	17.8	
2	574.0	98.84	65.75	11.5	42.2	
3	383.3	54.25	36.09	9.4	60.9	
4	773.3	84.14	55.98	7.2	59.2	
5	618.1	82.86	55.13	8.9	30.4	
6	399.6	94.52	62.88	15.7	152.1	
7	735.5	67.46	44.88	6.1	45.6	
8	1175.3	111.84	74.40	6.3	85.1	
Mean ± standard deviation	599.2 ± 312.7	90.4 ± 23.9	60.2 ± 15.9	16.2 ± 19.6	61.7 ± 41.9	

3.3. Vertical Nutrient Gradients

[25] All nutrient concentrations increased significantly below ~100 m depth though there were small and important vertical offsets in the depth at which each nutrient began to increase in concentration. In general, silicate concentrations begin to increase at 100 m depth, NO_3^- concentrations between 100 and 125 m depth, and PO_4^{3-} concentrations between 125 and 150 m depth. This vertical separation between the silicicline, nitracline, and phosphocline is not precise given the subjective criteria used to identify them but such depth offsets are recognized as important for the relative availability of different nutrients at the base of the euphotic zone [*Longhurst and Harrison*, 1989].

[26] Gradients in NO_3^- concentration at the top of the nitracline (the depth range over which concentrations begin to consistently increase) for all profiles measured during this cruise ranged from 3 to 190 μmol N m^{-4}, with a mean gradient of 25 ± 27 μmol N m^{-4}. These gradients are comparable to the mean gradient reported by *Mourino-Carballido et al*. [2011] of 62 ± 90 μmol N m^{-4} and to the range of gradients reported by *Painter et al*. [2008] of 33–124 μmol N m^{-4} for this region of the North Atlantic, though our mean gradient is somewhat lower than reported previously. We suspect that this is due to differences in where the nutrient gradient is calculated and sampling resolution between studies. To demonstrate this we present in Table 2 estimates of the nitracline gradient based on measurements taken at the top of the nitracline and on the basis of the maximum gradient in a particular profile, which was usually deeper than the top of the nitracline. Gradients at the top of the nitracline for the subset of eight stations we focus on here ranged from 5.48 to 44.5 μmol m^{-4} (mean 18.5 ± 12.1 μmol m^{-4}), whereas the maximum gradient ranged from 54.25 to 129.42 μmol m^{-4} (mean 90.4 ± 23.9 μmol m^{-4}). Both estimates are entirely consistent with previous observations but the notable increase in magnitude for the maximum gradient may help explain the ambiguity in interpreting previous nutrient flux estimates due to inconsistencies in the derivation of nitracline gradients (Figure 4; see section 4).

3.4. Ambient Diffusivity and Diffusive NO_3^- Fluxes

[27] Profiles of the Brunt-Väisälä buoyancy frequency, turbulent kinetic energy, and turbulent diffusivity from all 13 stations are presented in Figure 5 along with geometrically calculated (log transformed) cruise mean profiles. In general, the individual profiles were very similar to one another indicating minimal spatial or temporal variability. Over the depth range at which the nitracline was located (95–160 m) turbulent diffusivity within individual 8 m depth bins varied from 0.017 to 0.345 cm^2 s^{-1}. For an individual profile, the mean diffusivity calculated over the 95–160 m depth interval varied from 0.035 to 0.187 cm^2 s^{-1}. The cruise mean diffusivity over the 95–160 m depth interval was 0.077 ± 0.01 cm^2 s^{-1} (95% confidence interval limits 0.059–0.101 cm^2 s^{-1}) and comparable to existing estimates of open ocean diffusivity (e.g., 0.11 ± 0.02 cm^2 s^{-1}) [*Ledwell et al*., 1993]. This mean value appears to be 32% lower than that reported by *Ledwell et al*. [1993] but as the upper 95% confidence limit (0.101 cm^2 s^{-1}) approaches the value obtained by *Ledwell et al*. [1993] the two values are likely indistinguishable. In addition to estimating NO_3^- fluxes at the top of the nitracline we also define fluxes on the basis of the maximum nitracline gradient as this should provide an upper estimate of the magnitude of NO_3^- supply via turbulent diffusion. This is an important distinction as much of the ambiguity in flux estimates between different studies can be traced back to the depth, gradient, or approach used, which can broaden the

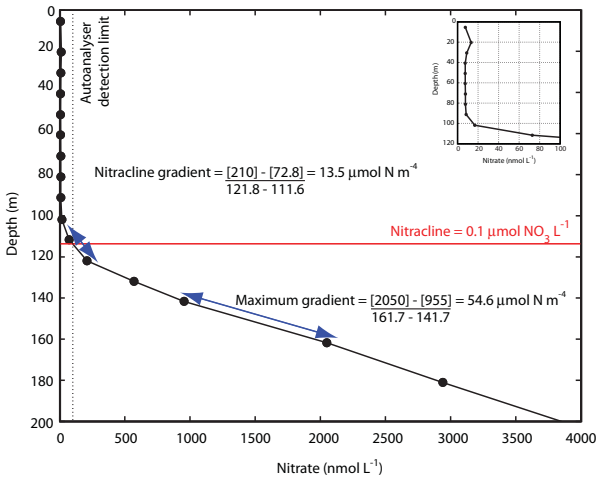

Figure 4. Schematic demonstrating the difference in nitracline gradient that may be calculated using different criteria. The gradient at the depth of the (arbitrarily) defined nitracline is almost four times smaller than the maximum gradient that may be derived from the same nutrient profile. Consequently, considerable variability may be introduced into the estimated nitrate flux. Interestingly, the maximum gradient is typically found near the base of the euphotic zone (0.1% surface PAR). Inset image shows nanomolar nutrient concentrations on a rescaled axis.

overall range of estimates because comparisons are not on a like-for-like basis.

[28] Turbulent diffusive NO_3^- fluxes at the top of the nitracline ranged from 3.65 to 29.61 µmol N m^{-2} d^{-1} and represent on average ~3% of the measurable NO_3^- demand in the overlying waters (Table 2). NO_3^- fluxes calculated using the maximum gradient ranged from 36.09 to 86.10 µmol N m^{-2} d^{-1} and, whilst larger, still only represented ~16% of the mean NO_3^- demand. With the exception of station 1 where the diffusive flux exceeded 60% of the measurable NO_3^- uptake, the diffusive flux of NO_3^- was typically <20% of the measured NO_3^- uptake (Table 2).

[29] The significance of N_2 fixation as a supply term was evaluated against the diffusive NO_3^- supply terms (Table 2). Depending upon how the nitracline gradient is defined our N_2 fixation observations could represent between 62% and 348% on average of the diffusive NO_3^- supply. Our preference is to utilize the maximum nitracline gradient as this will produce the largest potential flux of NO_3^-. Under this scenario, N_2 fixation represented between 18 and 152% of the diffusive NO_3^- flux and 62% on average. In other words, N_2 fixation was generally not as large a source of new nitrogen to the surface ocean as the diffusive NO_3^- flux, but neither was it an insignificant source.

3.5. Seasonal Context

[30] Modis Aqua sea surface temperature (SST) and surface chlorophyll data were analyzed to obtain the mean annual cycle for the eastern subtropical North Atlantic and to provide a seasonal context for our observations. In these waters, surface chlorophyll concentrations are typically <0.1 mg m^{-3} all year round but a weak seasonal cycle with a 2–3 fold variation in concentration is evident. Surface chlorophyll concentrations reach a typical annual maximum of ~0.08 mg m^{-3} during January to February, and a minimum concentration of ~0.04 mg m^{-3} in July to August (Figure 6). The mean MODIS chlorophyll concentration for the cruise period was 0.04 mg m^{-3} and was almost identical to the mean surface (5 m) chlorophyll concentration of 0.05 mg m^{-3} (range 0.03–0.08 mg m^{-3}) measured during the cruise. Based on the mean annual cycle shown in Figure 6, the annual mean surface chlorophyll concentration for these waters is 0.05 mg m^{-3}.

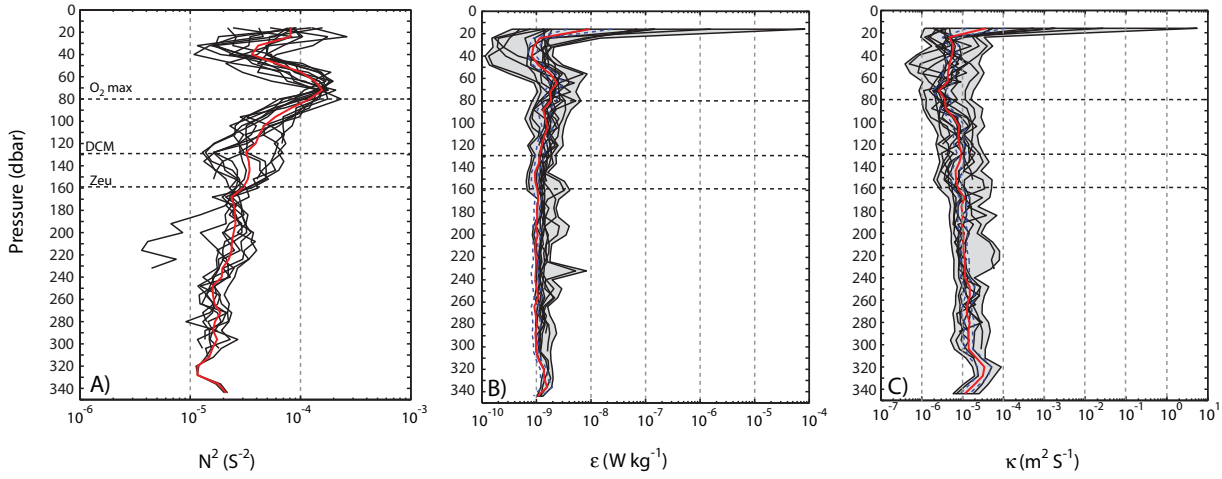

Figure 5. Vertical profiles (black lines) of (a) Brunt-Väisälä buoyancy frequency, (b) turbulent kinetic energy (ε), and (c) turbulent diffusivity (κ) collected from 13 stations in the eastern subtropical North Atlantic (~26.25°N, 31.1°W; see text for details). Gray shaded regions represent the envelope of 95% confidence intervals for the respective measurements. Thick red lines represent the cruise mean profile for each parameter and blue dashed lines the 95% confidence interval for the mean profile. Black dashed horizontal lines demark the cruise mean depth of the deep chlorophyll maximum (DCM), euphotic zone depth (Zeu; 0.1% surface irradiance), and oxygen maximum (O_2 max).

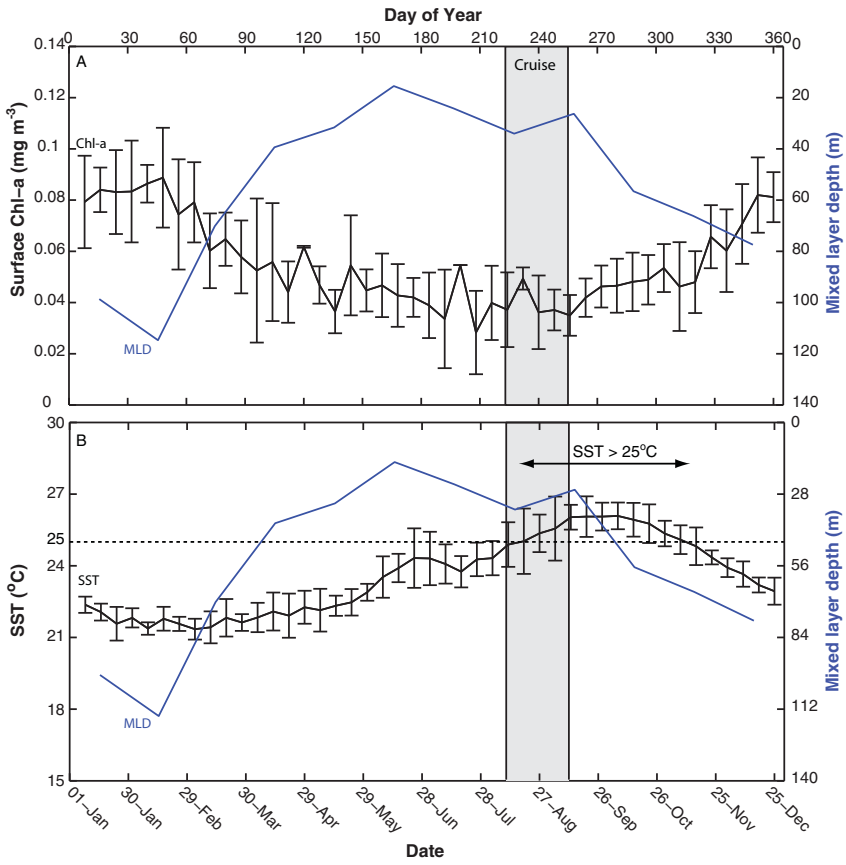

Figure 6. Annual cycle of (a) chlorophyll and (b) sea surface temperature for the eastern subtropical North Atlantic (based on observations centered around 26.25°N, 31.1°W). The annual chlorophyll cycle is calculated from Level 3 MODIS Aqua 8 day averaged chlorophyll data for the period 2002–2011 with error bars that represent the standard deviation of the mean calculated for each 8 day period from all available data points for that particular date over the data record. The annual SST cycle is derived from a similar MODIS Aqua Level 3 SST product for the same period with error bars representing the standard deviation of the mean. In both plots, the mixed layer depth (blue line) is derived from the ARGO based mixed layer climatology of *Hosoda et al*. [2010] and utilizes a density difference criteria of 0.03 kg m^{-3} relative to in situ density at 10 m. Note that Hosoda et al. provide monthly estimates of the mixed layer depth based on each full month of data and that in this figure the date of each mixed layer depth estimate has been reset to the middle of each month. The gray shaded region indicates the period of the present study.

[31] The annual cycle in SST is also shown in Figure 6. Maximum SSTs in excess of 26°C are typical from mid-September to early October, though temperatures generally exceed 25°C from mid-August through to mid-November. SST minima of ~22°C typically occur from late January through to late March. The climatological annual average SST for these waters is 23.5°C, which is warmer than the typical threshold temperature for *Trichodesmium* spp. of 20°C [*Capone et al*., 1997], although below the 24–30°C temperature range over which maximum growth rates are observed [*Breitbarth et al*., 2007]. The mean climatological MODIS SST for the cruise period was 25.3°C suggesting that ambient SSTs are usually optimal for maximum *Trichodesmium* growth at this time of year.

[32] In addition to mixed layer depth estimates calculated from cruise CTD casts, we also obtained the annual cycle in mixed layer depth for our study area from the ARGO mixed layer climatology of *Hosoda et al*. [2010]. The mixed layer depth was estimated using the same density threshold criteria of 0.03 kg $m^{\circ 3}$ relative to the density at 10 m [*de Boyer Montegut et al*., 2004]. The maximum mixed layer depth of ~120 m occurs in February/March, whilst the minimum mixed layer depth of ~20 m occurs in June. Despite the coincident timing of seasonal increases in mixed layer depth and in surface chlorophyll concentrations, it is still debated whether convective mixing during the cooler months is sufficiently deep enough to entrain significant quantities of nutrients to drive this change in chlorophyll concentration [*Beers et al*., 1982; *Hayward et al*., 1983; *Hayward*, 1987; *Dore et al*., 2008]. An alternative explanation of seasonal change in cellular chlorophyll content in response to seasonally changing irradiance intensities has also been suggested as a causal mechanism for the seasonal cycle in surface chlorophyll concentrations [*Winn et al*., 1995].

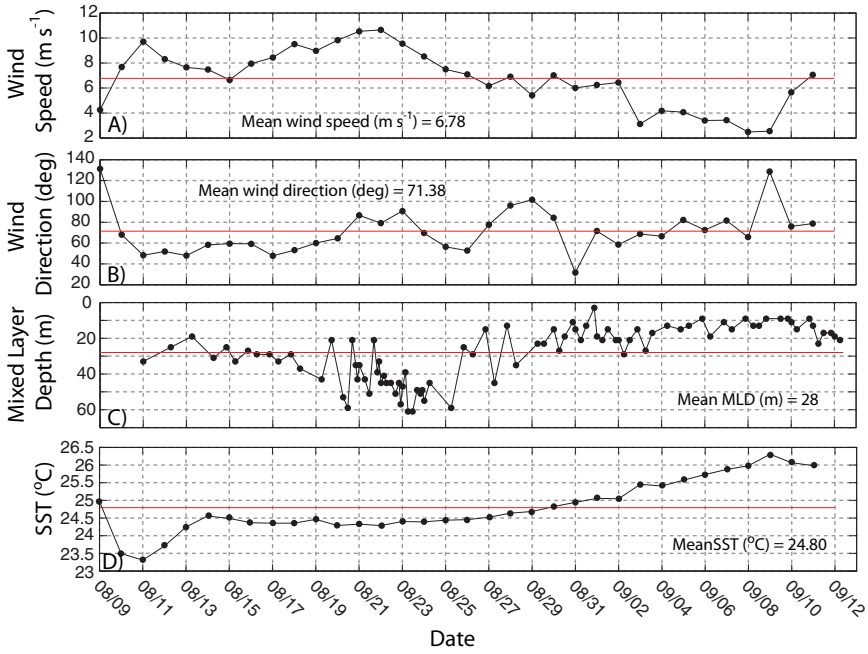

Figure 7. Local meteorological and surface ocean conditions. (a) Mean daily wind speed, (b) mean daily wind direction, (c) mixed layer depth, and (d) sea surface temperature. A prolonged reduction in the mean daily wind speed was evident from 22 August to 9 September during which time the mixed layer shoaled by almost 50 m and sea surface temperature increased by 2°C. The mixed layer depth was calculated from CTD profile data using a density threshold difference of 0.03 kg m^{-3} relative to in situ density at 10 m depth. Horizontal red lines represent the cruise mean for each parameter.

[33] In summary, our cruise during August and September took place during a period of relatively shallow mixed layer depths, low-surface chlorophyll concentrations, and high sea surface temperatures; conditions which should be preferential for diazotrophic organisms.

3.6. Intracruise Variability

[34] Throughout the preceding we have assumed environmental homogeneity throughout the cruise period. In Figure 7, we present observations of lower atmosphere and upper ocean variables measured during the cruise that reveal some important temporal changes during the observation period. It can be seen in Figure 7 that consistent gradual changes occurred to wind speeds (decreased from >8 m s^{-1} to <4 m s^{-1}), mixed layer depths (shoaled from >40 m to <20 m), and sea surface temperature (increased from <24.5°C to >26° C). The only variable for which there was no consistent change was wind direction, which was primarily east northeasterly ($\sim$71°). An analysis of air-mass back trajectories (Figure 8) confirms both the general wind direction, as well as also identifying key air mass source regions. In general, the air masses passing over the study site came from regions north of the study site and were typically oceanic in terms of their recent history. Two discrepancies to this generalization are apparent. First, between 10 and 14 August there appears to have been a shift in the air-mass source toward NW Europe, and second, between 25 and 29 August air with a distinctly African origin reached the study site.

[35] As both NW Europe and Africa can be important source regions for air-borne nutrient and iron deposition to the ocean we have attempted to ascertain what impact, if any, changes in wind direction may have had for our study particularly as sporadic rainfall (wet deposition) events were encountered and observed at a distance from the ship. Although no formal record of rainfall or of its nutrient and iron loading was made, the importance of wet deposition as a mechanism for introducing Saharan dust with its associated P and Fe content to the surface ocean requires consideration in the interpretation of our N_2 fixation results due to the positive effect such inputs can have on N_2 fixation rates and on the diazotrophic community [*Langlois et al*., 2012; *Benavides et al*., 2013]. A retrospective assessment of precipitation patterns over the study site was made possible by analysis of the NOAA Climate Prediction Centre's pentad (5 day) merged analysis of precipitation data set [*Xie and Arkin*, 1997]. This product is a global data set with a 2.5° resolution and consists of both direct-derived and satellite-derived precipitation rates, and whilst known to contain some inaccuracies [*Gruber et al*., 2000; *Xie et al*., 2003; *Yin et al*., 2004] is useful in the current context for demonstrating the timing of precipitation events. In Figure 9, we present a time series of the average daily precipitation rate for an area of the ocean approximating 23.75–28.75°N, 28.75–33.75°W, slightly larger than our study site. From this analysis, we identify a prominent precipitation event (Pmax) for the period of 19 August to 23 August, when precipitation reached 2.4 mm d^{-1}. This was followed by average daily precipitation rates of >0.8 mm d^{-1} for the period 24 August to 2 September. Whilst the overall precipitation rates are low by global standards, the increased precipitation between 19 August and 2 September followed minimal

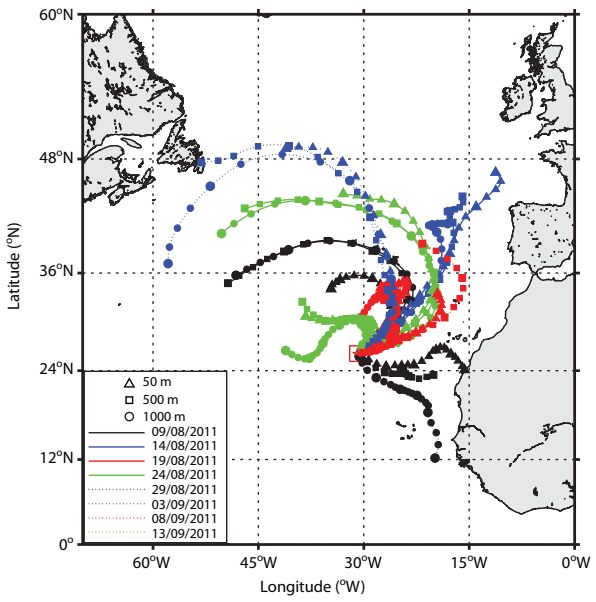

Figure 8. HYSPLIT air mass 5 day back trajectory results. Model runs (GDAS1 data set) were conducted at 5 day intervals to identify source regions that influenced the survey site (red box). Ship-based meteorological data indicate winds came from an average direction of 71° (ENE), comparable to HYSPLIT model results. The dominant source regions include W Atlantic, NW Europe, and NW Africa. Of interest here is the NW African source region identified as reaching the survey site on 29 August 2011, as air masses from this region have the potential to carry high dust loads to the remote open ocean.

precipitation (Pmin; <0.1 mm d^{-1}) for the preceding 2.5 months and was coincident with air-mass trajectories coming from Africa (Figure 8). We speculate therefore that the increase in precipitation coincident with the presence of an air mass from Africa increased the likelihood of P and Fe injection to the surface ocean during the observation period and thus represents a significant and important event that could explain some of the variability in our N_2 fixation rates.

4. Discussion

[36] We have reported new observations of N_2 fixation, NO_3^- uptake and turbulent diffusive NO_3^- supply from the oligotrophic eastern subtropical North Atlantic Ocean during the annual period of maximum sea surface temperatures and under variable meteorological conditions. In assessing the importance of these processes, we find that on average the diffusive NO_3^- flux represents <20% of the measurable NO_3^- uptake, implying the requirement for additional NO_3^- supply terms to balance the biological demand. A similar estimate of 18% can be obtained from the data presented by *Lewis et al*. [1986]. We also find that whilst N_2 fixation may indeed exceed the diffusive NO_3^- flux at an individual station, on average it was a smaller supply term and represented 62% of the diffusive NO_3^- supply. Against this background, the integrated rate of N_2 fixation equates to just 8% of integrated NO_3^- uptake rates (Table 2). Thus, whilst N_2 fixation may represent an important supply process for new nitrogen to the surface ocean the process of N_2 fixation itself is dwarfed in magnitude by the rate at which NO_3^- is consumed within these waters.

[37] To balance integrated rates of NO_3^- uptake an additional source (or sources) of NO_3^- other than turbulent diffusion must exist. Possible sources include lateral fluxes of NO_3^-, atmospheric inputs, mesoscale eddies, and nitrification. Simple calculations based on individual bottle samples indicate that the residence time for NO_3^- in the upper ocean varied from as little as 7 h to as long as 223 h (~9.3 days) with residence times increasing to as much as 626 h (26 days) within the upper nitracline. Therefore in order to maintain surface NO_3^- concentrations around the cruise mean value of ~7 nmol L^{-1} there has to have been a process supplying NO_3^- on a time scale of hours to days. Whilst the impact of lateral NO_3^- fluxes over the timescales required is considered minimal due to the lack of any significant horizontal gradients in NO_3^- concentrations within surface waters, the impact of mesoscale features is less obvious. *Johnson et al*. [2010] have highlighted the role of short-term input events in supplying NO_3^- to waters immediately above the nitracline but the mesoscale injection of NO_3^- was apparently not large enough to impact near surface (<50 m) concentrations as NO_3^- was rapidly consumed subsurface. We observed significant undulations in the nitracline, silicicline, and phosphocline between 100 and 150 m (Figure 3) suggesting that there were important mesoscale factors at work. Intriguingly, whilst there is some evidence to suggest moderately elevated concentrations of NO_3^-, $Si(OH)_4$, and PO_4^{3-} above the thermocline at several stations (Figure 3), there is little evidence to suggest that this supply mechanism was sufficient to impact near surface waters where NO_3^- residence times were typically <24 h.

[38] Atmospheric inputs of nitrogen to the ocean are generally considered to be poorly constrained due to a lack of observational data but such inputs are potentially significant in nitrogen-limited systems. *Baker et al*. [2010] estimate a typical atmospheric input (dry plus wet deposition) for NO_3^- and NH_4^+ of 21 µmol m^{-2} d^{-1} and 11.3 µmol m^{-2} d^{-1}, respectively, for the region of our study. In the

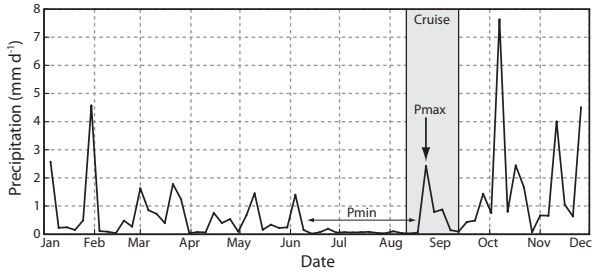

Figure 9. 2011 annual time series of precipitation for the region 23.75–28.75°N, 28.75–33.75° W. The period of the cruise is indicated by the gray box and the local maximum in precipitation (Pmax) is identified by an arrow. Pmin indicates the period of minimal precipitation prior to the cruise. This time series is based upon the NOAA Climate Prediction Centre Merged Analysis of Precipitation (CMAP) pentad product.

case of NO_3^-, this would equate to 3% or less of the integrated NO_3^- pool (Table 1) suggesting that the atmosphere is a generally less important source than the deep ocean [*Okin et al*., 2011]. However, depending upon the volume over which the atmospheric input is distributed the typical NO_3^- input suggested by *Baker et al*. [2010] may be locally significant. For example, if the total atmospheric input was evenly distributed over a 100 m water column this would equate to an input of 0.2 nmol L^{-1} d^{-1}, approximately 3% of the mean NO_3^- concentration of 7.1 nmol L^{-1} found over the upper 100 m. If, however, the atmospheric input was localized to a 10 m thick surface layer, the atmospheric input could equate to 2.1 nmol L^{-1} d^{-1} or ~30% of average in situ concentrations. Clearly, therefore, understanding how atmospheric inputs are distributed throughout the surface waters of the ocean is of particular importance for addressing any potential biological impact.

[39] Nitrification, the transformation of NH_4^+ to NO_3^-, is highly likely to be a major source of NO_2^- and NO_3^- in waters of the eastern subtropical North Atlantic but estimates of nitrification rates range widely [*Yool et al*., 2007; *Ward*, 2008]. In an exploratory study from the Atlantic Ocean, *Clark et al*. [2007] reported NH_4^+ and NO_2^- oxidation rates for a single irradiance depth (55% surface PAR) at a station located approximately 770 nmi north of our study site. The measured rates of NH_4^+ oxidation (0.05 nmol L^{-1} h^{-1}), and in particular of NO_2^- oxidation (0.45 nmol L^{-1} h^{-1}), were found to be sufficient to provide 270% of the local NO_3^- demand (0.17 nmol L^{-1} h^{-1}). In a more extensive study, *Clark et al*. [2008] reported NH_4^+ and NO_2^- oxidation rates for two irradiance depths (55 and 1% surface PAR) along a transect of the Atlantic Ocean. Rates of NH_4^+ oxidation were similar at both depth horizons ranging from 0 to 10 nmol L^{-1} d^{-1}, whereas NO_2^- oxidation rates increased from 0.4 to 12 nmol L^{-1} d^{-1} at 55% PAR to 1–31 nmol L^{-1} d^{-1} at the base of the euphotic zone. These rates were sufficient to turnover all inorganic nitrogen pools (NH_4^+, NO_2^- NO_3^-) on a subdaily timescale.

[40] The mean NO_3^- uptake rate for our observations made between the surface and the deep chlorophyll maximum was equivalent to 4.6 nmol L^{-1} d^{-1}, almost identical to the mean NO_2^- oxidation rate of 4.7 nmol L^{-1} d^{-1} reported by *Clark et al*. [2008] for depths equivalent to 55% PAR. Therefore, typical nitrification rates within the upper euphotic zone appear more than capable of providing the NO_3^- needed to support observed uptake rates and may easily account for the additional 80% needed to support our integrated uptake rates once the contribution from diffusion is accounted for. If, however, NO_2^- oxidation rates approach the higher mean value of 13.2 nmol L^{-1} d^{-1} as reported for the base of the euphotic zone by *Clark et al*. [2008], then nitrification alone could provide almost three times as much NO_3^- as is consumed on a daily basis. Clearly, under a steady-state assumption a sustained contribution of this magnitude over and above in situ demand would lead to an accumulation of NO_3^- in surface waters that may account for some of the variability in surface NO_3^- concentrations reported in previous studies [*Painter et al*., 2008] but the breadth of existing nitrification observations is too small to explore this possibility further.

[41] *Mourino-Carballido et al*. [2011] reported simultaneous measurements of diffusive NO_3^- flux and N_2 fixation in the subtropical North Atlantic which indicated that N_2 fixation could provide only 2% of the nitrogen supplied by diffusive NO_3^- fluxes across the nitracline. This appears to be the result of an unusually high diffusivity term of 5 cm^2 s^{-1}, roughly 65 times larger than we observed, but also due to rates of N_2 fixation that were lower (11 ± 9 μmol N m^{-2} d^{-1}) than those we report here. As the observations reported by *Mourino-Carballido et al*. [2011] were made in April and May, when sea surface temperatures can be 3–4°C cooler (Figure 6), it is perhaps not surprising that N_2 fixation rates were lower but the cause of the higher diffusivity term is less clear. Nitracline gradients reported by *Mourino-Carballido et al*. [2011] are similar to those we report here which indicates that the difference in diffusivity is a key factor behind the low supply from N_2 fixation reported by *Mourino-Carballido et al*. [2011]. A number of possible explanations for this exist including spurious data, temporal and spatial variability and differences in methodologies for the calculation of diffusivity, which may all singularly or collectively explain the disparity in the significance of N_2 fixation in these waters. Independent measurements of turbulent diffusivity from the wider subtropical North Atlantic tend to provide diffusivities closer to 0.1 cm^2 s^{-1} [*Lewis et al*., 1986; *Ledwell et al*., 1993, 1998, 2008] but diffusivities >1 cm^2 s^{-1} are known from studies in the subpolar North Atlantic [*Law et al*., 2001; *Jickells et al*., 2008]. It would appear therefore that the assessment of the importance of N_2 fixation reported by *Mourino-Carballido et al*. [2011] and in this study are not directly comparable due to both seasonal differences in N_2 fixation rates and important differences in the magnitude of the diffusivity term.

4.1. A Synthesis of Previous Observations

[42] Our principal observations of N_2 fixation, NO_3^- uptake and of the nitracline gradient are central to the question of how important N_2 fixation is as a supply mechanism of new nitrogen to the subtropical North Atlantic. More fundamentally, however, we must first assess how representative our observations are for the eastern subtropical North Atlantic.

[43] We present in Figure 10 an assessment of the maximum nitracline gradient calculated from 12 separate cruise data sets collected over a 13 year period (1995–2008) as part of the Atlantic Meridional Transect (www.amt-uk.org) [*Robinson et al*., 2006]. Cruises were conducted in boreal spring or autumn months and show broad similarities in the maximum nitracline gradient between 24 and 36°N. There, gradients rarely exceeded 200 μmol m^{-4} and more typically were <100 μmol m^{-4}, which suggests weak interannual variability. Differences in cruise track and occasional sampling within the NW African upwelling system (~20°N) can produce distinctly sharper nitracline gradients. Influence from upwelling near the equatorial region further south has a similar effect. Generally, all cruises show reduced variability in the nitracline gradient between 24 and 36°N. Three cruises shown in Figure 10 are more directly comparable to the present study (the others are influenced to differing degrees by the NW African upwelling system as a result of differences in cruise transect). These three cruises

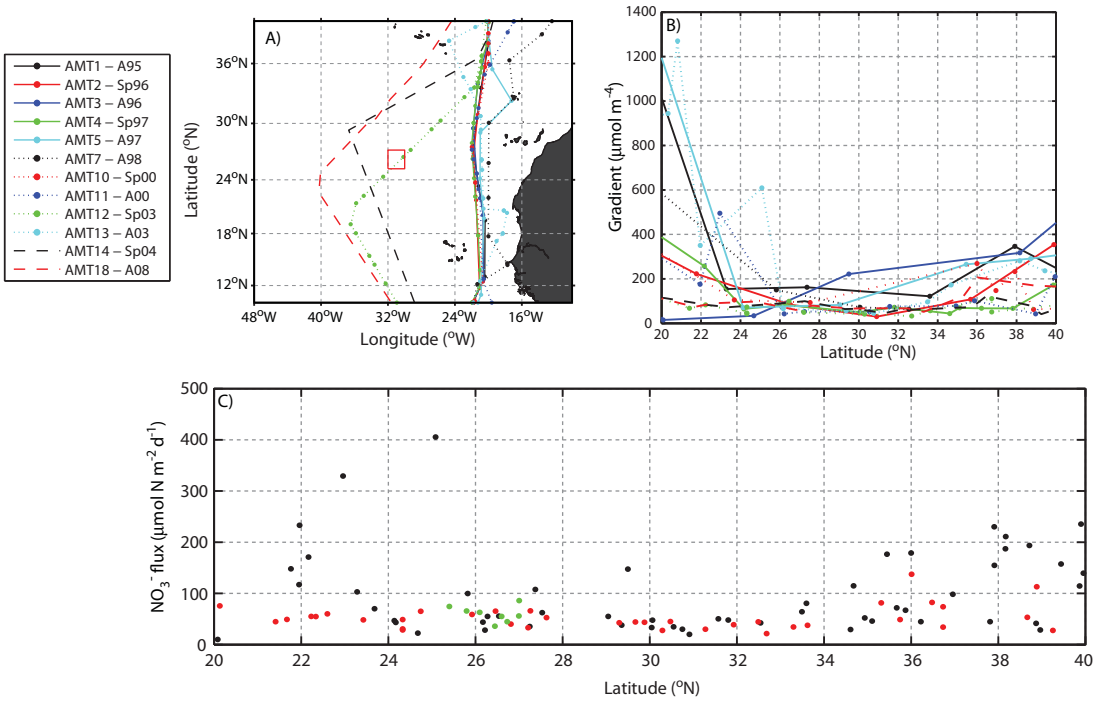

Figure 10. Observations of nitracline gradients and NO_3^- fluxes in the eastern subtropical North Atlantic from the Atlantic Meridional Transect (AMT) program made between 1995 and 2008. In (a) we present the various AMT cruise transects and station positions from which vertical profiles of NO_3^- were collected. In (b) we present the maximum nitracline gradients obtained for each profile. In (c) we present the resulting NO_3^- fluxes calculated using the mean diffusivity obtained in the present study (red box in Figure 10a; 0.077 $cm^2\ s^{-1}$). Note that differences in cruise transects and the influence of the NW African upwelling system is evident in the nitracline gradient data thus negating a truthful examination of seasonal or interannual variability in NO_3^- fluxes. However, three cruises (AMT12, AMT14, and AMT18) sampled the open waters of the eastern subtropical North Atlantic and are more appropriate comparisons to the present study; these cruises are indicated by the red dots in Figure 10c, the present study is shown in green. In the legend, the year of each cruise and the boreal season during cruise departure are abbreviated, thus A95 indicates Autumn 1995, Sp96 Spring 1996, and so on.

produce mean nitracline gradients of 63 ± 24 μmol NO_3^- m^{-4} (AMT12), 78 ± 24 μmol NO_3^- m^{-4} (AMT14), and 96 ± 48 μmol NO_3^- m^{-4} (AMT18) for stations between 24 and 36°N. These mean gradients are very comparable to the mean gradient of the present study (90 ± 24 μmol NO_3^- m^{-4}; Table 2) suggesting that nitracline gradients are relatively well constrained in this region to between 50 and 100 μmol NO_3^- m^{-4}. Using the individual gradients obtained from the AMT data set presented in Figure 10 in conjunction with the mean diffusivity of 0.077 $cm^2\ s^{-1}$ obtained in the present study, we thus obtain NO_3^- fluxes which are generally <100 μmol NO_3^- $m^{-2}\ d^{-1}$ (Figure 10).

[44] In Figure 11, we present a synthesis of NO_3^- uptake rates from previous studies in the eastern subtropical North Atlantic. Though there is quite often some considerable difference in the choice of integration depth between studies (examples range from 20 to 180 m) and in the sampling resolution (3–8 depths), there is nevertheless a broad agreement both in terms of the magnitude of the integrated NO_3^- pool and in terms of the integrated NO_3^- uptake rates. Estimates of the integrated NO_3^- pool vary from 0.2 to 166 mmol NO_3^- m^{-2} (mean 36 mmol NO_3^- m^{-2}), with one exceptional estimate of 857 mmol NO_3^- m^{-2} reported by *Varela et al.* [2005] which appears to derive from the location of this station being close to the NW African upwelling system and correspondingly high NO_3^- concentrations at depth. In the context of these previous observations, our estimates of the integrated NO_3^- pool of 0.72–17.95 mmol NO_3^- m^{-2} are comparable (Table 1 and Figure 11). The same general conclusion is true of our NO_3^- uptake rates (0.13–1.18 mmol N $m^{-2}\ d^{-1}$) (Table 1), which are within the range of previous estimates of 0.06–34 mmol NO_3^- $m^{-2}\ d^{-1}$ (mean 3.15 mmol NO_3^- $m^{-2}\ d^{-1}$) (Figure 11). Finally, we note a disparity between the common assumption for the seasonal increase in surface chlorophyll (Figure 3), which is considered due to the seasonal entrainment of NO_3^- from the nitracline when the surface mixed layer deepens in winter, and the data assembled here. There is no suggestion of seasonality in either the integrated NO_3^- pool or in NO_3^- uptake rates to support the assumption that increased NO_3^- concentrations underlie enhanced chlorophyll concentrations (Figure 11). There is, however, a significant temporal bias underlying the observations which cluster around year day 150 (late May) and year days 260–280 (September to October) which limits this temporal assessment and there appears to be surprisingly little information in the literature regarding NO_3^- uptake during the boreal winter months for this region.

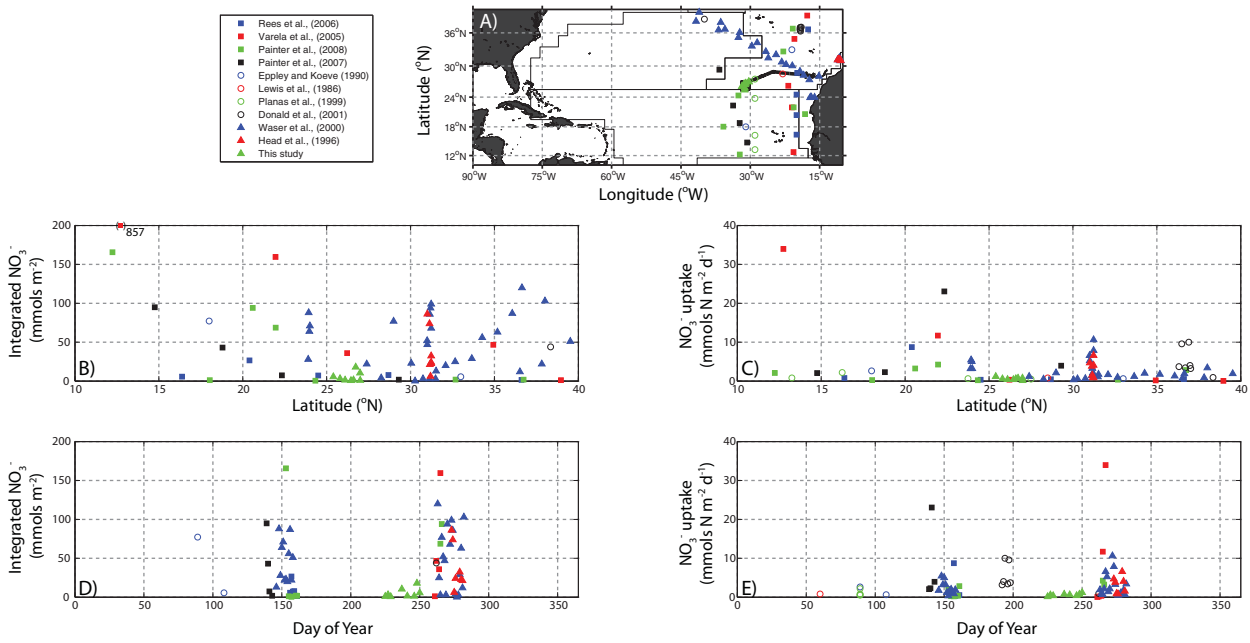

Figure 11. Synthesis of previous studies in the eastern subtropical North Atlantic (10–45°W, 10–40°N) where both integrated NO_3^- pools and integrated NO_3^- uptake rates have been obtained. (a) The position of previous observations used in this analysis along with the static boundaries of Longhurst Provinces [*Longhurst*, 1998]; the cruise track of the present study is represented by the black line. In (b) and (d) we show the range of integrated NO_3^- pools observed by the various studies against latitude and day of year, respectively. Note that in Figure 11b one observation lies beyond the *y* axis limits and is denoted along with its concentration along the top axis. In (c) and (e) we show integrated rates of NO_3^- uptake against latitude and day of year, respectively. It is evident that despite wide spatial coverage observations remain rather sparse through time and are typically clustered during the year with the majority of observations being obtained in June and September. Individual data sourced from *Lewis et al*. [1986], *Eppley and Koeve* [1990], *Head et al*. [1996], *Planas et al*. [1999], *Waser et al*. [2000], *Donald et al*. [2001], *Varela et al*. [2005], *Rees et al*. [2006], and *Painter et al*. [2007, 2008].

[45] A global synthesis of N_2 fixation rates has recently been made available [*Luo et al*., 2012] and we utilize this database to assess our observations. Our study site is located in the middle of a region of relatively low N_2 fixation rates (Figure 12) compared to the higher rates that are more typical nearer the equator [*Moore et al*., 2009]. This is most likely due to relatively low surface iron concentrations in this region [*Rijkenberg et al*., 2011, 2012] and more broadly to the impact iron has on rates of N_2 fixation [*Mills et al*., 2004; *Moore et al*., 2009]. Our measurements of surface N_2 fixation rates are comparable to previous observations (Figure 12), though our integrated rates can be higher. This suggests that general undersampling is responsible for an incomplete picture of the range and interannual variability of integrated N_2 fixation rates in this sector of the northeast subtropical Atlantic Ocean.

4.2. Methodological Caveats

[46] In the context of previous observations from the eastern subtropical North Atlantic there is no suggestion that our rate measurements or NO_3^- flux estimates are atypical. The only parameter that we are unable to fully constrain is the ambient diffusivity, but the majority of existing observations tend to constrain this value closer to $\sim$0.1 $cm^2\ s^{-1}$ than to 1 $cm^2\ s^{-1}$. Thus, it is highly unlikely that the conclusions we reach above regarding the importance of N_2 fixation (62% of the diffusive flux) are significantly in error. However, despite its wide usage the $^{15}N_2$ "bubble" technique introduced by *Montoya et al*. [1996] has recently come under increased scrutiny amid concern that the technique underestimates N_2 fixation rates [*Mohr et al*., 2010]. These concerns were subsequently investigated by *Großkopf et al*. [2012] using a technique similar to that first used by *Dugdale et al*. [1959, 1961] in which a preprepared seawater solution containing dissolved $^{15}N_2$ is added to a seawater sample as a solution rather than a gas. This approach removes the assumption that the injected bubble of $^{15}N_2$ equilibrates with the sample and harmonizes the technique to existing stable isotope methodologies in which the tracer is added as a solution. Using the method of *Mohr et al*. [2010], *Großkopf et al*. [2012] reported elevated N_2 fixation rates in the Atlantic Ocean compared to rates obtained with the bubble technique of *Montoya et al*. [1996]. In particular *Großkopf et al*. [2012] report an average increase in N_2 fixation rates of 62% compared to parallel results with the existing bubble technique. The full extent of a methodological underestimate of N_2 fixation rates on global nitrogen budgets requires a great deal of further observational study but *Großkopf et al*. [2012] estimate that the global N_2 fixation rate could increase by $\sim$70% to 177 $\pm$ 8 Tg N yr^{-1}. In a related study, *Wilson et al*. [2012] compared the N_2 bubble technique, the N_2 solution

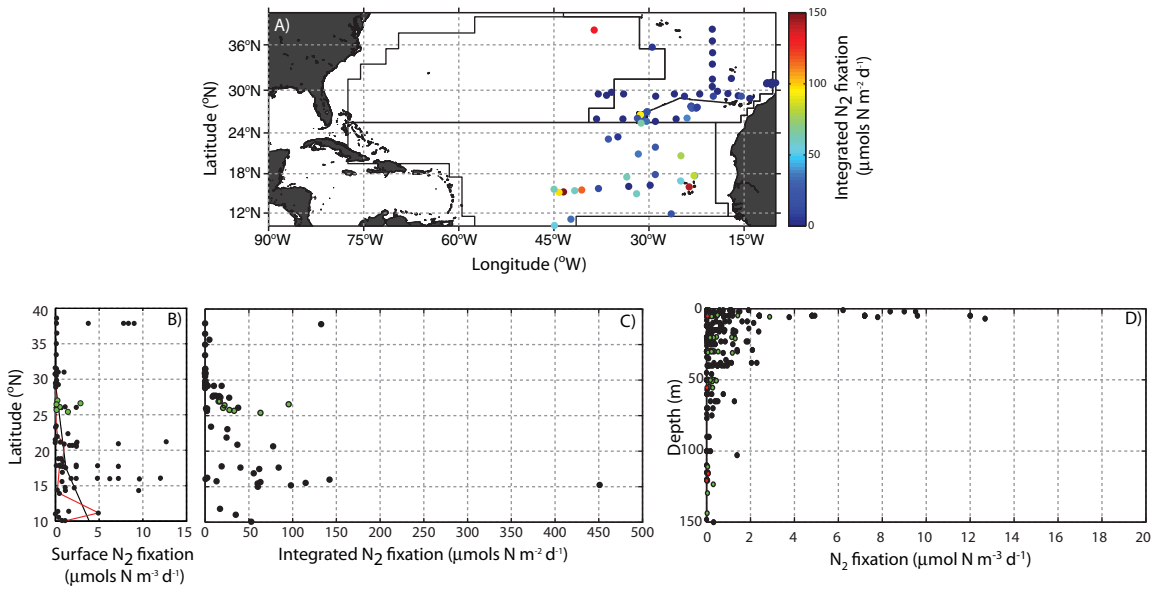

Figure 12. N_2 fixation measurements collated from the literature and as measured in this study. (a) The positions of profiles of N_2 fixation extracted from the database compiled by *Luo et al*. [2012] for the eastern subtropical North Atlantic (10–45°W, 10–40°N). The cruise track of the preset study is represented by the black line. (b) Surface (<10 m) N_2 fixation rates from the database and we highlight two recent meridional surveys [*Moore et al*., 2009] black line and [*Mourino-Carballido et al*., 2011] red line which indicate the low-latitude maxima in surface N_2 fixation rates; note that the *x* axis scale has been restricted to highlight the low N_2 fixation rates that are typical of the study region and that two results with fixation rates of ∼150 μmol m^{-3} d^{-1} are excluded from this figure. (c) Integrated N_2 fixation rates against latitude, which again highlights the low-latitude maxima that is typical of the North Atlantic. In (d), we present profiles of volumetric N_2 fixation rates highlighting the typical near surface maxima in N_2 fixation. In Figures 12b–12d, black dots represent literature observations, green (total) and red (<8 μm size fraction) dots represent the results of this study. All data extracted from the synthesis present by *Luo et al*. [2012] with individual data coming from studies reported by *Benavides et al*. [2011], *Capone et al*. [2005], *Fernandez et al*. [2010], *Mourino-Carballido et al*. [2011], *McCarthy and Carpenter* [1979], *Moore et al*. [2009], *Turk et al*. [2011], *Goebel et al*. [2010], *Rees et al*. (unpublished data), and *Mulholland et al*. (unpublished data).

technique, and the alternative acetylene reduction technique [*Stewart et al*., 1967], and independently confirmed that the popular N_2 bubble technique does indeed lead to significant underestimates of N_2 fixation rates compared to the solution technique. Furthermore, *Wilson et al*. [2012] also highlight deficiencies in the acetylene reduction technique, particularly the use of a fixed conversion ratio between the amount of acetylene reduced and the amount of nitrogen fixed. Consequently, at the present time the historical record of N_2 fixation measurements must be viewed with caution and our best estimates of global N_2 fixation rates derived from these measurements as underestimates.

[47] In this study, we used the $^{15}N_2$ bubble technique and whilst our N_2 fixation results compare well to previous observations (Figure 12), the bulk of which are based on the N_2 bubble and acetylene reduction assays, growing recognition of methodological problems with the most commonly used method suggests that the historical record is less reliable than thought and that the level of uncertainty over regional and global N_2 fixation rates is probably higher than we would like. Although *Großkopf et al*. [2012] found that the makeup of the underlying diazotroph community was critical in explaining the magnitude of the difference in the results of the two techniques, with *Trichodesmium* dominated communities producing smaller methodological differences, we cannot say with certainty what error is present in our results as we do not have a full description of the diazotrophic community. Our study region was located at the northern edge of the region recognized as receiving Saharan dust inputs (the Saharan dust belt 10°S–25° N), further north than the abundance maxima for *Trichodesmium* (∼10°N) [*Moore et al*., 2009], located in a region where SST exceeds 25°C only seasonally (Figure 6), and in a region where nitrogenase (*nifH*) expression suggests a diverse diazotrophic population is present [*Turk et al*., 2011]. Consequently, it is highly probable that our N_2 fixation rates are low. The few size-fractionated N_2 fixation results we have, suggest that N_2 fixation by the <8 µm fraction, which was typically ∼10 µmol N m^{-2} d^{-1} (Table 1), represented between 27 and 67% of the total measurable N_2 fixation rate and thus any error may be significant. Interestingly, *Großkopf et al*. [2012] found that the methodological discrepancy was at a regional minimum at 25°N (their supplementary Figure 5), which may lower rather than increase the unquantified error in our results.

[48] Assuming our measured N_2 fixation rates are low by 62% (the average underestimate reported by *Großkopf et al*. [2012]) we have recalculated the importance of N_2 fixation relative to our NO_3^- flux term (Table 2). The results suggest that for an individual comparison N_2 fixation could represent between 29 and 246% of the NO_3^- flux with a mean value of 100%. Under this scenario, it would appear that N_2 fixation balances and frequently exceeds the diffusive flux of NO_3^- in the eastern subtropical North Atlantic. Recognition of the increase in both the importance and magnitude of N_2 fixation rates will benefit on-going attempts at closing regional nitrogen budgets, particularly for the subtropical ocean where the discrepancy between the rates of nitrogen supply and geochemical estimates of nitrogen demand has remained unresolved for almost three decades. Combined with an important role for carbon export [*Karl et al*., 2012], N_2 fixation is likely to continue to redefine our understanding of the marine nitrogen cycle in the years ahead.

[49] **Acknowledgments.** We thank C. M. Moore and D. Honey for technical advice, M. Bolshaw and D. Spanner (all University of Southampton) and A. Rees and L. Al-Moosawi (Plymouth Marine Laboratory) for assistance with the isotopic analyses, Y.-W. Luo (Woods Hole Oceanographic Institute) for providing access to the global diazotrophic database of *Luo et al*. [2012], S. van Gennip, V. Paba, R. Green, and J. Allen for assistance with the turbulence profiler at sea and the Natural Environment Research Council for supporting this work through the Oceans 2025 research program. We also thank the two reviewers for their constructive comments. This study benefited from access to the extensive AMT database (http://www.amt-uk.org/) and is a contribution to the international IMBER project and was supported by the UK Natural Environment Research Council National Capability funding to Plymouth Marine Laboratory and the National Oceanography Centre, Southampton. This is contribution 238 of the AMT program.

References

Baker, A. R., T. Lesworth, C. Adams, T. D. Jickells, and L. Ganzeveld (2010), Estimation of atmospheric nutrient inputs to the Atlantic Ocean from 50°N to 50°S based on large-scale field sampling: Fixed nitrogen and dry deposition of phosphorus, *Global Biogeochem. Cycles*, *24*, GB3006, doi:10.1029/2009GB003634.

Beers, J. R., F. M. H. Reid, and G. L. Stewart (1982), Seasonal abundance of the microplankton population in the North Pacific central gyre, *Deep Sea Res., Part A*, *29*(2), 227–245.

Benavides, M., N. S. R. Agawin, J. Aristegui, P. Ferriol, and L.J. Stal (2011), Nitrogen fixation by Trichodesmium and small diazotrophs in the subtropical northeast Atlantic, *Aquat. Microb. Ecol.*, *65*, 43–53.

Benavides, M., J. Aristegui, N. S. R. Agawin, J. L. Cancio, and S. Hernandez-Leon (2013), Enhancement of nitrogen fixation rates by unicellular diazotrophs vs. Trichodesmium after a dust deposition event in the Canary Islands, *Limnol. Oceanogr.*, *58*(1), 267–275.

Bibby, T. S., and C. M. Moore (2011), Silicate:nitrate ratios of upwelled waters control the phytoplankton community sustained by mesoscale eddies in sub-tropical North Atlantic and Pacific, *Biogeosciences*, *8*, 657–666.

Breitbarth, E., A. Oschlies, and J. LaRoche (2007), Physiological constraints on the global distribution of Trichodesmium—Effect of temperature on diazotrophy, *Biogeosciences*, *4*, 53–61.

Capone, D. G., J. A. Burns, J. P. Montoya, A. Subramaniam, C. Mahaffey, T. Gunderson, A. F. Michaels, and E. J. Carpenter (2005), Nitrogen fixation by Trichodesmium spp.: An important source of new nitrogen to the tropical and subtropical North Atlantic Ocean, *Global Biogeochem. Cycles*, *19*, GB2024, doi:10.1029/2004GB002331.

Capone, D. G., J. P. Zehr, H. W. Paerl, B. Bergman, and E. J. Carpenter (1997), Trichodesmium, a globally significant marine cyanobacterium, *Science*, *276*, 1221–1229.

Carpenter, E. J., and D. G. Capone (2008), Nitrogen fixation in the marine environment, in *Nitrogen in the Marine Environment*, 2nd ed., edited by D. G. Capone et al., pp. 141–198, Academic Press, San Diego, Calif.

Clark, D. R., A. P. Rees, and I. Joint (2007), A method for the determination of nitrification rates in oligotrophic marine seawater by gas chromatography/mass spectrometry, *Mar. Chem.*, *103*, 84–96.

Clark, D. R., A. P. Rees, and I. Joint (2008), Ammonium regeneration and nitrification rates in the oligotrophic Atlantic Ocean: Implications for new production estimates, *Limnol. Oceanogr.*, *53*(1), 52–62.

de Boyer Montegut, C., G. Madec, A. S. Fischer, A. Lazar, and D. Ludicone (2004), Mixed layer depth over the global ocean: An examination of profile data and a profile-based climatology, *J. Geophys. Res.*, *109*, C12003, doi:10.1029/2004JC002378.

Deutsch, C., J. L. Sarmiento, D. M. Sigman, N. Gruber, and J. P. Dunne (2007), Spatial coupling of nitrogen inputs and losses in the ocean, *Nature*, *445*, 163–167.

DeVries, T., C. Deutsch, F. Primeau, B. Chang, and A. Devol (2012), Global rates of water-column denitrification derived from nitrogen gas measurements, *Nat. Geosci.*, *5*, 547–550.

Donald, K. M., I. Joint, A. P. Rees, E. M. S. Woodward, and G. Savidge (2001), Uptake of carbon, nitrogen and phosphorus by phytoplankton along the 20 degrees W meridian in the NE Atlantic between 57.5 degrees N and 37 degrees N, *Deep Sea Res., Part II*, *48*(4–5), 873–897.

Dore, J. E., R. M. Letelier, M. J. Church, R. Lukas, and D. M. Karl (2008), Summer phytoplankton blooms in the oligotrophic North Pacific Subtropical Gyre: Historical perspective and recent observations, *Prog. Oceanogr.*, *76*, 2–38.

Dugdale, R. C., and J. J. Goering (1967), Uptake of new and regenerated forms of nitrogen in primary productivity, *Limnol. Oceanogr.*, *12*(2), 196–206.

Dugdale, R. C., and F. P. Wilkerson (1986), The use of 15N to measure nitrogen uptake in eutrophic oceans: Experimental considerations, *Limnol. Oceanogr.*, *31*(4), 673–689.

Dugdale, R., V. Dugdale, J. Neess, and J. Goering (1959), Nitrogen fixation in lakes, *Science*, *130*, 859–860.

Dugdale, R., D. W. Menzel, and J. H. Ryther (1961), Nitrogen fixation in the Sargasso Sea, *Deep Sea Res.*, *7*, 297–300.

Eppley, R. W., and W. Koeve (1990), Nitrate use by plankton in the eastern subtropical North Atlantic, March–April 1989, *Limnol. Oceanogr.*, *35*(8), 1781–1178.

Fernandez, A., B. Mourino-Carballido, A. Bode, M. Varela, and E. Maranon (2010), Latitudinal distribution of Trichodesmium spp. and N_2 fixation in the Atlantic Ocean, *Biogeosciences*, *7*, 3167–3176.

Forryan, A., A. P. Martin, M. A. Srokosz, E. E. Popova, S. C. Painter, and M. C. Stinchcombe (2012), Turbulent nutrient fluxes in the Iceland Basin, *Deep Sea Res., Part I*, *63*, 20–35.

Forryan, A., A. P. Martin, M. A. Srokosz, E. E. Popova, S. C. Painter, and A. H. Renner (2013), A new observationally motivated Richardson number based mixing parameterization for oceanic mesoscale flows, *J. Geophys. Res.*, *118*, 1–15, doi:10.1002/jgrc.20108.

Goebel, N. L., K. A. Turk, K. M. Achilles, R. Paerl, I. Hewson, A. E. Morrison, J. P. Montoya, C. A. Edwards, and J. P. Zehr (2010), Abundance and distribution of major groups of diazotrophic cyanobacteria and their potential contribution to N_2 fixation in the tropical Atlantic Ocean, *Environ. Microbiol.*, *12*(12), 3272–3289.

Großkopf, T., W. Mohr, T. Baustian, H. Schunck, D. Gill, M. M. M. Kuypers, G. Lavik, R. A. Schmitz, D. W. R. Wallace, and J. LaRoche (2012), Doubling of marine dinitrogen-fixation rates based on direct measurements, *Nature*, *488*, 361–364.

Gruber, A., X. Su, M. Kanamitsu, and J. Schemm (2000), The comparison of two merged rain gauge-satellite precipitation datasets, *Bull. Am. Meteorol. Soc.*, *81*(11), 2631–2644.

Gruber, N. (2008), The marine nitrogen cycle: Overview and challenges, in *Nitrogen in the Marine Environment*, 2nd ed., edited by D. G. Capone et al., pp. 1–50, Academic Press, San Diego, Calif.

Gruber, N., and J. L. Sarmiento (1997), Global patterns of marine nitrogen fixation and denitrification, *Global Biogeochem. Cycles*, *11*(2), 235–266.

Harrison, W. G. (1990), Nitrogen utilization in chlorophyll and primary productivity maximum layers: An analysis based on the f-ratio, *Mar. Ecol. Prog. Ser.*, *60*, 85–90.

Hayward, T. L. (1987), The nutrient distribution and primary production in the central North Pacific, *Deep Sea Res.*, *34*(9), 1593–1627.

Hayward, T. L. (1991), Primary production in the North Pacific Central Gyre: A controversy with important implications, *Trends Ecol. Evol.*, *6*(9), 281–284.

Hayward, T. L. (1994), The shallow oxygen maximum layer and primary production, *Deep Sea Res., Part I*, *41*(3), 559–574.

Hayward, T. L., E. L. Venrick, and J. A. McGowan (1983), Environmental heterogeneity and plankton community structure in the central North Pacific, *J. Mar. Res.*, *41*, 711–729.

Head, E. J. H., W. G. Harrison, B. I. Irwin, E. P. W. Horne, and W. K. W. Li (1996), Plankton dynamics and carbon flux in an area of upwelling off the coast of Morocco, *Deep Sea Res., Part I*, *43*(11–12), 1713–1738.

Hosoda, S., T. Ohira, K. Sato, and T. Suga (2010), Improved description of global mixed-layer depth using Argo profiling floats, *J. Oceanogr.*, *66*, 773–787.

Jenkins, W. J. (1982), Oxygen utilization rates in North Atlantic subtropical gyre and primary production in oligotrophic systems, *Nature*, *300*, 246–248.

Jickells, T. D., et al. (2008), A Lagrangian biogeochemical study of an eddy in the Northeast Atlantic, *Prog. Oceanogr.*, *76*, 366–398.

Johnson, K. S., S. C. Riser, and D. M. Karl (2010), Nitrate supply from deep to near-surface waters of the North Pacific subtropical gyre, *Nature*, *465*, 1062–1065.

Karl, D., R. Letelier, L. Tupas, J. Dore, J. Christian, and D. Hebel (1997), The role of nitrogen fixation in biogeochemical cycling in the subtropical North Pacific Ocean, *Nature*, *388*(6642), 533–538.

Karl, D., A. Michaels, B. Bergman, D. Capone, E. Carpenter, R. Letelier, F. Lipschultz, H. Paerl, D. Sigman, and L. Stal (2002), Dinitrogen fixation in the world's oceans, *Biogeochemistry*, *57/58*(1), 47–98.

Karl, D. M., and R. M. Letelier (2008), Nitrogen fixation-enhanced carbon sequestration in low nitrate, low chlorophyll seascapes, *Mar. Ecol. Prog. Ser.*, *364*, 257–268.

Karl, D. M., M. J. Church, J. E. Dore, R. M. Letelier, and C. Mahaffey (2012), Predictable and efficient carbon sequestration in the North Pacific Ocean supported by symbiotic nitrogen fixation, *Proc. Natl. Acad. Sci. U. S. A.*, doi:10.1073/pnas.1120312109.

Kirk, J. T. O. (2010), *Light and Photosynthesis in Aquatic Ecosystems*, 649 p., Cambridge Univ. Press, Cambridge.

Kirkwood, D. S. (1996), Nutrients: Practical notes on their determination in seawater, *ICES Techniques in Marine Environmental Sciences Report*, *17*, 25 pp., International Council for the Exploration of the Seas, Copenhagen.

Langlois, R. J., M. M. Mills, C. Ridame, P. Croot, and J. LaRoche (2012), Diazotrophic bacteria respond to Saharan dust additions, *Mar. Ecol. Prog. Ser.*, *470*, 1–14.

Law, C. S., A. P. Martin, M. I. Liddicoat, A. J. Watson, K. J. Richards, and E. M. S. Woodward (2001), A Lagrangrian SF_6 tracer study of an anticyclonic eddy in the North Atlantic: Patch evolution, vertical mixing and nutrient supply to the mixed layer, *Deep Sea Res., Part II*, *48*, 705–724.

Le Bouteiller, A. (1986), Environmental control of nitrate and ammonium uptake by phytoplankton in the Equatorial Atlantic Ocean, *Mar. Ecol. Prog. Ser.*, *30*, 167–179.

Ledwell, J. R., A. J. Watson, and C. S. Law (1993), Evidence for slow mixing across the pycnocline from an open-ocean tracer-release experiment, *Nature*, *364*, 701–703.

Ledwell, J. R., D. J. McGillicuddy Jr., and L. A. Anderson (2008), Nutrient flux into an intense deep chlorophyll layer in a mode-water eddy, *Deep Sea Res., Part II*, *55*, 1139–1160.

Ledwell, J. R., A. J. Watson, and C. S. Laws (1998), Mixing of a tracer in the pycnocline, *J. Geophys. Res.*, *103*(C10), 21,499–21,529.

Lewis, M. R., W. G. Harrison, N. S. Oakey, D. Herbert, and T. Platt (1986), Vertical nitrate fluxes in the oligotrophic ocean, *Science*, *234*, 870–873.

Lipschultz, F., N. R. Bates, C. A. Carlson, and D. A. Hansell (2002), New production in the Sargasso Sea: History and current status, *Global Biogeochem. Cycles*, *16*(1), 1001, doi:10.1029/2000GB001319.

Longhurst, A. (1998), *Ecological Geography of the Sea*, Academic, San Diego, Calif.

Longhurst, A. R., and W. G. Harrison (1989), The biological pump: Profiles of plankton production and consumption in the upper ocean, *Prog. Oceanogr.*, *22*, 47–123.

Luo, Y.-W., et al. (2012). Database of diazotrophs in global ocean: Abundance, biomass and nitrogen fixation rates, *Earth Syst. Sci. Data*, *4*, 47–73.

Mahaffey, C., A. F. Michaels, and D. G. Capone (2005), The conundrum of marine N_2 fixation, *Am. J. Sci.*, *305*, 546–595.

Maranon, E., P. M. Holligan, M. Varela, B. Mourino, and A. J. Bale (2000), Basin-scale variability of phytoplankton biomass, production and growth in the Atlantic Ocean, *Deep Sea Res., Part I*, *47*(5), 825–857.

McCarthy, J. J., and E. J. Carpenter (1979), Oscillatoria (Trichodesmium) thiebautii (cyanophyta) in the central North Atlantic Ocean, *J. Phycol.*, *15*(1), 75–82, doi:10.1111/j.1529–8817.1979.tb02965.x.

Mills, M. M., C. Ridame, M. Davey, J. L. Roche, and R. J. Geider (2004), Iron and phosphorous co-limit nitrogen fixation in the eastern tropical North Atlantic, *Nature*, *429*, 292–294.

Mohr, W., T. Großkopf, D. W. R. Wallace, and J. LaRoche (2010), Methodological underestimation of oceanic nitrogen fixation rates, *PLoS One*, *5*(9), e12583.

Montoya, J. P., M. Voss, P. Kahler, and D. G. Capone (1996), A simple, high-precision, high-sensitivity tracer assay for N_2 fixation, *Appl. Environ. Microbiol.*, *62*(3), 986–993.

Moore, C. M., et al. (2009), Large-scale distribution of Atlantic nitrogen fixation controlled by iron availability, *Nat. Geosci.*, *2*, 867–871, doi:10.1038/NGEO1667.

Moum, J. N., M. Gregg, R. Lien, and M. Carr (1995), Comparison of turbulence kinetic-energy dissipation rate estimates from 2 ocean microstructure profilers, *J. Atmos. Oceanic Technol.*, *12*, 346–366.

Mourino-Carballido, B., R. Grana, A. Fernandez, A. Bode, M. Varela, J. F. Dominguez, J. Escanez, D. d. Armas, and E. Maranon (2011), Importance of N_2 fixation vs. nitrate eddy diffusion along a latitudinal transect in the Atlantic Ocean, *Limnol. Oceanogr.*, *56*(3), 999–1007.

Mulholland, M. R., and M. W. Lomas (2008), Nitrogen uptake and assimilation, in *Nitrogen in the Marine Environment*, 2nd ed., edited by D. G. Capone et al., pp. 303–384, Academic Press, San Diego, Calif., doi: 10.1016/B978-0-12-372522-6.00007-4.

Okin, G. S., et al. (2011), Impacts of atmospheric nutrient deposition on marine productivity: Roles of nitrogen, phosphorus, and iron, *Global Biogeochem. Cycles*, *25*, GB2022, doi: 10.1029/2010GB003858.

Osborn, T. R. (1980), Estimates of the local rate of vertical diffusion from dissipation measurements, *J. Phys. Oceanogr.*, *10*, 83–89.

Painter, S. C., R. Sanders, A. J. Poulton, E. M. S. Woodward, M. Lucas, and K. Chamberlain (2007), Nitrate uptake at photic zone depths is not important for export in the subtropical ocean, *Global Biogeochem. Cycles*, *21*, GB4005, doi:10.1029/2006GB002807.

Painter, S. C., R. Sanders, H. N. Waldron, M. I. Lucas, E. M. S. Woodward, and K. Chamberlain (2008), Nitrate uptake along repeat meridional transects of the Atlantic Ocean, *J. Mar. Syst.*, *74*, 227–240.

Patey, M. D., E. P. Achterberg, M. J. A. Rijkenberg, P. J. Statham, and M. Mowlem (2010), Interferences in the analysis of nanomolar concentrations of nitrate and phosphate in oceanic waters, *Anal. Chim. Acta*, *673*, 109–116.

Patey, M. D., M. J. A. Rijkenberg, P. J. Statham, M. C. Stinchcombe, E. P. Achterberg, and M. Mowlem (2008), Determination of nitrate and phosphate in seawater at nanomolar concentrations, *Trends Anal. Chem.*, *27*(2), 169–182.

Perez, V., E. Fernandez, E. Maranon, X. Anxelu, G. Moran, and M. V. Zubkov (2006), Vertical distribution of phytoplankton biomass, production and growth in the Atlantic subtropical gyres, *Deep Sea Res., Part I*, *53*, 1616–1634.

Planas, D., S. Agusti, C. M. Duarte, T. C. Granata, and M. Merino (1999), Nitrate uptake and diffusive nitrate supply in the Central Atlantic, *Limnol. Oceanogr.*, *44*(1), 116–126.

Poulton, A. J., R. Sanders, P. M. Holligan, M. C. Stinchcombe, T. R. Adey, L. Brown, and K. Chamberlain (2006), Phytoplankton mineralization in the tropical and subtropical Atlantic Ocean, *Global Biogeochem. Cycles*, *20*, GB4002, doi:10.1029/2006GB002712.

Rees, A. P., E. M. S. Woodward, and I. Joint (2006), Concentrations and uptake of nitrate and ammonium in the Atlantic Ocean between 60°N and 50°S, *Deep Sea Res., Part II*, *53*(14–16), 1649–1665.

Rijkenberg, M. J. A., R. J. Langlois, M. M. Mills, M. D. Patey, P. G. Hill, M. C. Nielsdottir, T. J. Compton, J. LaRoche, and E. P. Achterberg (2011), Environmental forcing of nitrogen fixation in the eastern tropical and sub-tropical North Atlantic Ocean, *PLoS One*, *6*(12), 1–13, e28989.

Rijkenberg, M. J. A., S. Steigenberger, C. F. Powell, H. v. Haren, M. D. Patey, A. R. Baker, and E.P. Achterberg (2012), Fluxes and distribution of dissolved iron in the eastern (sub-) tropical North Atlantic Ocean, *Global Biogeochem. Cycles*, *26*, GB3004, doi:10.1029/2011GB004264.

Rippeth, T., J. Simpson, E. Williams, and M. Inall (2003), Measurement of the rates of production and dissipation of turbulent kinetic energy in an energetic tidal flow: Red Wharf Bay revisited, *J. Phys. Oceanogr.*, *33*, 1889–1901.

Robinson, C., et al. (2006). The Atlantic Meridional Transect (AMT) Programme: A contextual view 1995–2005, *Deep Sea Res., Part II*, *53*(14–16), 1485–1515.

Singh, A., M. W. Lomas, and N. R. Bates (2013), Revisiting N_2 fixation in the North Atlantic Ocean: Significance of deviations from the Redfield Ratio, atmospheric deposition and climate variability, *Deep Sea Res., Part II*, *93*, 148–158, doi:10.1016/j.dsr2.2013.04.008.

Stewart, W. D. P., G. P. Fitzgerald, and R. H. Burris (1967), In situ studies on N2 fixation, using the acetylene reduction technique, *Proc. Natl. Acad. Sci. U. S. A.*, *58*, 2071–2078.

Stips, A. (2005), Dissipation measurements, in *Marine Turbulence: Theories, Observations and Models, Results of the CARTUM Project*, edited by H. Baumert and J. Simpson, pp. 115–126, Cambridge Univ. Press, Cambridge.

Subramaniam, A., C. Mahaffey, W. Johns, and N. Mahowald (2013), Equatorial upwelling enhances nitrogen fixation in the Atlantic Ocean, *Geophys. Res. Lett.*, *40*, 1766–1771, doi:10.1002/grl.50250.

Turk, K. A., A. P. Rees, J. P. Zehr, N. Pereira, P. Swift, R. Shelley, M. Lohan, E. M. S. Woodward, and J. Gilbert (2011), Nitrogen fixation and nitrogenase (nifH) expression in tropical waters of the eastern North Atlantic, *ISME J.*, *5*, 1201–1212.

Varela, M. M., A. Bode, E. Fernandez, N. Gonzalez, V. Kitidis, M. Varela, and E. M. S. Woodward (2005), Nitrogen uptake and dissolved organic nitrogen release in planktonic communities characterised by phytoplankton size-structure in the Central Atlantic Ocean, *Deep Sea Res., Part I*, *52*, 1637–1661.

Venrick, E. L., J. A. McGowan, and A. W. Mantyla (1973), Deep maxima of photosynthetic chlorophyll in the Pacifc Ocean, *Fish. Bull.*, *71*(1), 41–52.

Ward, B. B. (2008), Nitrification in marine systems, in *Nitrogen in the Marine Environment*, 2nd ed., edited by D. G. Capone et al., pp. 199–261, Academic Press, San Diego, Calif.

Waser, N. A. D., W. G. Harrison, E. J. H. Head, B. Nielsen, V. A. Lutz, and S. E. Calvert (2000), Geographic variations in the nitrogen isotope composition of surface particulate nitrogen and new production across the North Atlantic Ocean, *Deep Sea Res., Part I*, *47*, 1207–1226.

Welch, P. (1967), The use of fast fourier transform for the estimation of power spectra: A method based on time averaging over short, modified periodograms, *IEEE Trans. Audio Electroacoust.*, *15*(2), 70–73.

Welschmeyer, N. A. (1994), Fluorometric analysis of chlorophyll a in the presence of chlorophyll b and phaeopigments, *Limnol. Oceanogr.*, *39*(8), 1985–1992.

Wilson, S. T., D. Bottjer, M. J. Church, and D. M. Karl (2012), Comparative assessment of nitrogen fixation methodologies conducted in the oligotrophic North Pacific Ocean, *Appl. Environ. Microbiol.*, *78*(18), 6516–6523, doi:10.1128/AEM.01146-12.

Winn, C. D., L. Campbell, J. R. Christian, R. M. Letelier, D. V. Hebel, J. E. Dore, L. Fujieki, and D. M. Karl (1995), Seasonal variability in the phytoplankton community of the North Pacific Subtropical Gyre, *Global Biogeochem. Cycles*, *9*(4), 605–620.

Wu, J., W. Sunda, E. A. Boyle, and D. M. Karl (2000), Phosphate depletion in the western North Atlantic Ocean, *Science*, *289*, 759–762.

Xie, P., and P.A. Arkin (1997), Global precipitation: A 17-year monthly analysis based on gauge observations, satellite estimates and numerical model outputs, *Bull. Am. Meteorol. Soc.*, *78*(11), 2539–2558.

Xie, P., J. E. Janowiak, P. A. Arkin, R. Adler, A. Gruber, R. Ferraro, G. J. Huffman, and S. Curtis (2003), GPCP pentad preciptation analyses: An experimental dataset based on gauge observations and satellite estimates, *J. Clim.*, *16*, 2197–2214.

Yamazaki, H., and T. Osborn (1990), Dissipation estimates for stratified turbulence, *J. Geophys. Res.*, *95*, 9739–9744.

Yin, X., A. Gruber, and P. Arkin (2004), Comparison of the GPCP and CMAP merged gauga-satellite monthly precipitation products for the period 1979–2001, *J. Hydrometeorol.*, *5*, 1207–1222.

Yool, A., A. P. Martin, C. Fernandez, and D. R. Clark (2007), The significance of nitrification for oceanic new production, *Nature*, *447*, 999–1002.